NASA TECHNICAL NOTE

NASA TN D-7180

NASA TN D-7180

AN ANALYSIS OF A CHARRING ABLATOR WITH THERMAL NONEQUILIBRIUM, CHEMICAL KINETICS, AND MASS TRANSFER

by Ronald K. Clark

Langley Research Center
Hampton, Va. 23365

NATIONAL AERONAUTICS AND SPACE ADMINISTRATION • WASHINGTON, D. C. • JUNE 1973

1. Report No. NASA TN D-7180	2. Government Accession No.	3. Recipient's Catalog No.
4. Title and Subtitle AN ANALYSIS OF A CHARRING ABLATOR WITH THERMAL NONEQUILIBRIUM, CHEMICAL KINETICS, AND MASS TRANSFER		5. Report Date 6. Performing Organization Code June 1973
7. Author(s) Ronald K. Clark		8. Performing Organization Report No. L-8670
9. Performing Organization Name and Address NASA Langley Research Center Hampton, Va. 23665		10. Work Unit No. 502-37-02-01 11. Contract or Grant No.
12. Sponsoring Agency Name and Address National Aeronautics and Space Administration Washington, D.C. 20546		13. Type of Report and Period Covered Technical Note 14. Sponsoring Agency Code

15. Supplementary Notes Part of the information presented herein was included in a thesis entitled "A Numerical Analysis of the Transient Response of an Ablation System Including Effects of Thermal Non-Equilibrium, Mass Transfer and Chemical Kinetics" submitted in partial fulfillment of the requirements for the degree of Doctor of Philosophy in Mechanical Engineering at Virginia Polytechnic Institute and State University, Blacksburg, Virginia, May 1972.

16. Abstract

The differential equations governing the transient response of a one-dimensional ablative thermal protection system are presented for the general case of thermal nonequilibrium between the pyrolysis gases and the char layer and with finite rate chemical reactions occurring in the char layer. The system consists of three layers – the char layer, the uncharred layer, and an optional insulation layer – with concentrated heat sinks at the back surface and between the second and third layers. The equations are solved numerically by using a modified implicit finite-difference scheme to obtain solutions for the thickness of the charred and uncharred layers, surface-recession and pyrolysis rates, solid temperatures, porosity profiles, and profiles of pyrolysis-gas temperature, pressure, composition, and flow rate.

Good agreement is obtained between numerical results and exact solutions for a number of simplified cases.

The complete numerical analysis is used to obtain solutions for an ablative system subjected to a constant heating environment. Effects of thermal, chemical, and mass-transfer processes are shown.

17. Key Words (Suggested by Author(s)) Ablation Heat transfer Mass transfer	18. Distribution Statement Unclassified – Unlimited		
19. Security Classif. (of this report) Unclassified	20. Security Classif. (of this page) Unclassified	21. No. of Pages 76	22. Price* $3.00

*For sale by the National Technical Information Service, Springfield, Virginia 22151

AN ANALYSIS OF A CHARRING ABLATOR WITH THERMAL NONEQUILIBRIUM, CHEMICAL KINETICS, AND MASS TRANSFER*

By Ronald K. Clark
Langley Research Center

SUMMARY

An analysis is presented for predicting the transient response of a one-dimensional ablative thermal protection system to a high-energy air environment. The mathematical equations are presented for the general case of a three-layer charring ablator system (char layer, uncharred layer, and insulation layer) undergoing oxidation and/or sublimation at the heated surface with homogeneous and heterogeneous chemical reactions occurring within the char layer and with a finite rate of heat transfer between the char layer and the pyrolysis gases flowing through the char (that is, the pyrolysis gases and char layer may not be in thermal equilibrium). The equations are solved numerically by using a modified implicit finite-difference scheme to obtain solutions for the thickness of the charred and uncharred layers, surface-recession and pyrolysis rates, solid temperatures, char-layer porosity profiles, and profiles of pyrolysis-gas temperature, pressure, composition, and flow rate.

Good agreement is obtained between numerical results and exact solutions for a charring ablator system subjected to a constant heating environment. Effects of thermal, chemical, and mass-transfer processes are pronounced. Also, results shown herein compare numerical solutions from this analysis with solutions from a previous analysis which did not treat the chemical and mass-transfer processes as thoroughly as this analysis. This analysis predicts that the overall performance for a low-density phenolic-nylon ablator is 16 percent greater than the performance indicated by the previous analysis. The difference in predicted performance results from consideration of char-layer deposition in this analysis.

The calculations presented herein are for a phenolic-nylon charring ablator system. However, since no restriction regarding the type of material was made in deriving the governing equations, this analysis is capable of handling other ablation materials when proper data are used.

---

*Part of the information presented herein was included in a thesis entitled "A Numerical Analysis of the Transient Response of an Ablation System Including Effects of Thermal Non-Equilibrium, Mass Transfer and Chemical Kinetics" submitted in partial fulfillment of the requirements for the degree of Doctor of Philosophy in Mechanical Engineering at Virginia Polytechnic Institute and State University, Blacksburg, Virginia, May 1972.

INTRODUCTION

The analysis of ablative heat shields has been the subject of research for over 10 years. As a result of that research many analyses are available for making heat-shield calculations. References 1 to 4 show that, in general, the capability exists for treating the following:

(1) Multilayer systems

(2) Energy balance at the external surface with convective and radiative heat input and energy blocking by mass injection

(3) Interaction of the external surface with the boundary-layer fluid resulting in surface removal by oxidation, sublimation, and mechanical erosion

(4) Heat transfer internally by conduction and convection

(5) In-depth pyrolysis of the uncharred layer

(6) Internal chemical reactions with mass deposition

(7) Mass-transfer processes represented by quasi-steady-state equations

(8) Thermal equilibrium between the pyrolysis gas and the char layer

Experimental and numerical results presented in references 5 and 6 show that the chemical processes and mass deposition in the char layer are extensive and that a significant temperature difference between the pyrolysis gas and the char layer may exist. Thus these results show that items (7) and (8) represent limitations of the existing analyses. This paper presents an analysis which describes the transient response of an ablative thermal protection system undergoing ablation, including a detailed treatment of the various thermal, chemical, and mass-transfer processes present in ablation. Differential equations governing heat and mass transfer for both the char layer and the pyrolysis gases flowing through the char layer are used. These equations are coupled through a convective-heat-transfer term which represents energy transfer between the char layer and the pyrolysis gases. The differential equation governing the pressure distribution in the char layer is also used as are the equations describing the chemical reactions occurring in the char layer.

The governing equations are solved numerically by using a digital computer. Numerical solutions are obtained for a number of simplified problems, for which exact solutions can be obtained, to test the accuracy of various parts of the total program. Results are presented for an ablator subjected to a constant heating rate with surface removal by oxidation and finite-rate chemistry occurring in the char layer to illustrate the effects of thermal, chemical, and mass-transfer processes in ablation. A comparison is also made of these results with results obtained by using the analysis of reference 4.

The governing equations necessary for a detailed description of ablation processes are complex and computer solutions of these equations are time consuming. Thus, the objectives of this program are to develop the capability of analyzing ablation systems including some higher order effects, to provide the capability of studying effects of these higher order parameters on ablative performance, and to provide a means of calibrating existing less complex analyses to account for those effects which are found to be significant.

SYMBOLS

A	radiant-energy absorption of char layer, W/m^3
A'	specific reaction-rate constant for pyrolysis of uncharred material, kg/m^2-sec
$[A_i]$	mole density of chemical species i, g-mol/m^3
A_S	specific surface area (area per unit volume) of char layer, 1/m; specific reaction-rate constant for surface removal by oxidation (various units)
B'	activation energy for pyrolysis of uncharred layer, K
B_S	activation energy for surface removal by oxidation, K
C	mass fraction of oxygen in boundary layer
C_p	heat capacity at constant pressure, J/g-mol-K
C_S	solid carbon
D	diffusion coefficient, m^2/sec
E	radiant-energy emission of char layer, W/m^3
E_1,E_2,E_3	coefficients in linearized differential equation for char-layer porosity
H	enthalpy, J/g-mol
H_A	volumetric convective-heat-transfer coefficient, W/m^3-K

H_c heat of sublimation of char layer, J/kg

$H(T)$ enthalpy at temperature T, J/g-mol

I number of finite-difference stations in char layer

J number of finite-difference stations in uncharred layer

K permeability of char layer, m^2; number of finite-difference stations in insulation layer

K_h constant in equation for H_A (eq. (7)), 1/m

k reaction rate of chemical reaction (various units); thermal conductivity, W/m-K

l thickness, m

M molecular weight, kg/g-mol

$\dot{m}$ mass-flow rate, kg/m^2-sec

$\dot{m}_{O_2}$ mass rate of diffusion of O_2 through boundary layer to char-layer surface, kg/m^2-sec

$\dot{m}_s$ mass rate of char removal, kg/m^2-sec

$\dot{m}_T$ effective rate of mass injection into boundary layer, kg/m^2-sec

N_{Le} dimensionless parameter, $k/\rho C_p D$ (Lewis number)

N_{Pr} dimensionless parameter, $\mu C_p/k$ (Prandtl number)

n order of chemical reaction

n(r) parameter defined by equation (11b)

P Laplace transform of ϕ defined by $\int_0^\infty e^{-St}\phi(x',t)dt$; pressure, N/m^2

q	rate of energy transfer, W/m^2
q_{AERO}	net aerodynamic-heating rate to surface, W/m^2
q_B	net heating rate to back surface of insulation layer, W/m^2
q_C	cold-wall convective-heating rate to front surface, W/m^2
$q_{C,net}$	net convective-heating rate to front surface, W/m^2
q_R	radiant-heating rate to front surface, W/m^2
q_s'''	rate of energy generated in solid by sources, W/m^2
R	molar rate of production by chemical reactions, $g\text{-}mol/m^3\text{-}sec$
R_u	universal gas constant, J/g-mol-K
r	rate of progress of chemical reaction, $1/m^3\text{-}sec$
S	dummy parameter used in equation (C9)
$S\left(T_{s,1} - \overline{T}_1\right)$	step function defined by equation (23)
T	temperature, K
$\overline{T}_I$	maximum temperature of pyrolysis zone used when limiting temperature at that station, K
$\overline{T}_1$	maximum char-surface temperature used when limiting temperature at that station, K
t	time, sec
$\bar{V}_c$	velocity of finite-difference station in moving coordinate system, m/sec
v	velocity of pyrolysis gases in char layer, m/sec
v_o	superficial velocity of pyrolysis gases in char layer, m/sec

x	dimensionless moving coordinate
x'	parameter defined by equation (C8b)
x_i	mole fraction of chemical species i
y	fixed coordinate, m
z	fixed coordinate, m
α	absorptance of front surface
α_c	weighting factor for char material injected into boundary layer
α_p	weighting factor for pyrolysis gases injected into boundary layer
$\alpha_1,\alpha_2,\alpha_3,\alpha_4$	coefficients in linearized differential equation for solid temperature
β	trigger for selecting blocking approximation: $\beta = 0$ for second-order approximation; $\beta = 1$ for linear approximation
β_1,β_2,β_3	coefficients in linearized differential equation for pyrolysis-gas temperature
$\gamma_1,\gamma_2,\gamma_3,\gamma_4$	coefficients in linearized differential equation for pyrolysis-gas pressure
$\Delta_{1,i},\Delta_{2,i},\Delta_{3,i}$	coefficients in linearized chemical-species conservation equation
ΔH	heat of reaction for heterogeneous chemical reaction
ΔH_c	heat of combustion of char, J/g-mol
ΔH_p	heat of pyrolysis of uncharred material, J/kg
$\Delta\rho$	difference in density of uncharred material and char layer at pyrolysis zone, kg/m^3
ϵ_s	emittance of char surface

ϵ''_s emittance of back surface

η porosity

$\bar{\eta}$ blocking coefficient used with linear ablation theory

θ_i fraction of surface sites occupied by molecules of chemical species i

θ_o fraction of surface sites which are void

λ ratio of char-layer mass removed to mass of oxygen diffusing to surface

μ viscosity of pyrolysis gases or boundary-layer fluid, N-sec/m^2

ν'_i coefficient of chemical species i appearing as reactant in stoichiometric representation of chemical reaction, g-mol

ν''_i coefficient of chemical species i appearing as product in stoichiometric representation of chemical reaction, g-mol

ρ density, kg/m^3

$\rho_{s,0}$ density of char layer at front surface, kg/m^3

σ Stefan-Boltzmann constant, W/m^2-sec-K^4

ϕ dimensionless temperature defined by equation (C8a)

Superscripts:

' uncharred layer

'' insulation layer

P at start of time step

P+Δt at end of time step

P+(Δt/2) at middle of time step

r	chemical reaction r

Subscripts:

CO	carbon monoxide
C_s	solid carbon
c	oxidation
e	edge of boundary layer
f	forward direction
g	pyrolysis gas
HS	heat sink between uncharred layer and insulation layer
HSP	heat sink at back surface
h	heterogeneous chemical reaction
I	pyrolysis zone
I+J	interface of uncharred layer and insulation layer
I+J+K	back surface of insulation layer
i	chemical species i
N	station N
O_2	oxygen
o	initial value; reservoir condition
r	reverse direction
s	solid

sb	sublimation
T	total value
w	wall
x=0	at char surface
x=1	at pyrolysis zone
1	char-layer surface

Overlines:

-	normalized or average
^	per unit mass

ANALYSIS

Figure 1 shows a schematic diagram of a charring ablator system consisting of a char layer, pyrolysis zone, uncharred layer, and insulation layer. The heated front surface of the char layer interacts with the external boundary layer resulting in erosion of the char layer. The uncharred layer degrades at the pyrolysis zone and the products of pyrolysis flow through the char layer absorbing energy and undergoing homogeneous and/or heterogeneous chemical reactions. If heterogeneous reactions are involved, deposition or internal erosion will occur and the char-layer density is affected. Thus a description of the char layer (a porous solid through which pyrolysis gases flow) requires conservation equations for energy in the solid and the gas, momentum of the gas, chemical species, total mass, and an equation for porosity variation.

The pyrolysis zone is considered to be a plane of zero thickness in this analysis. Reference 7 shows good agreement between numerical solutions for char-layer temperatures obtained with a plane pyrolysis zone and with in-depth pyrolysis. The assumption of a plane pyrolysis zone was necessary in this analysis to provide a second boundary condition for the gas-momentum conservation equation.

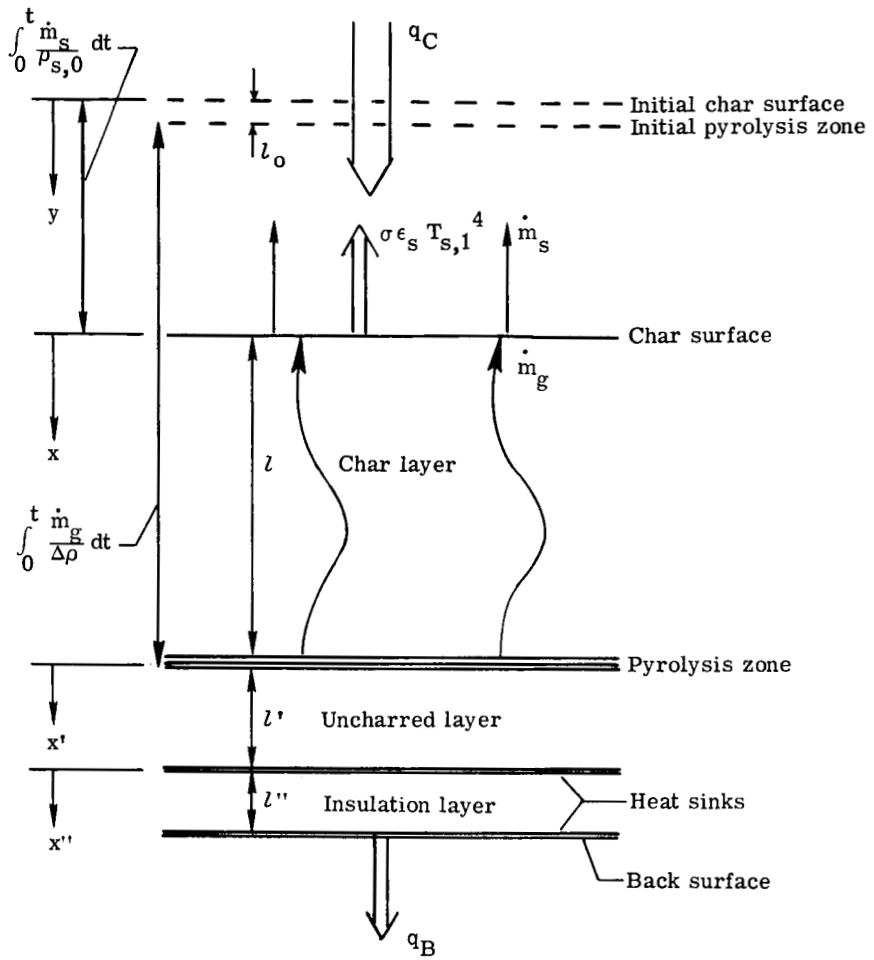

Figure 1.- Schematic diagram of charring ablator with coordinates.

Governing Equations

The equations describing the performance of a charring ablator system are derived in reference 8. These equations, written for one dimension in space, and neglecting viscous dissipation, gas-phase conduction, diffusion, and external forces, are now given.

Char-layer equations.- The char temperature equation is

$$(1 - \eta)\frac{\rho_s C_{p,s}}{M_s}\frac{\partial T_s}{\partial t} = \frac{\partial}{\partial y}\left(k_s \frac{\partial T_s}{\partial y}\right) - H_A(T_s - T) + \eta R_s\left[\overline{H(T)}\right]_s + \eta R_{h,s} H_s - \eta \sum_r r_h^{(r)} \Delta H^{(r)}$$

$$+ (1 - \eta)(A - E) + (1 - \eta)q_s''' + \frac{\rho_s H_s}{M_s}\frac{\partial \eta}{\partial t} \qquad (1)$$

The pyrolysis-gas pressure equation is

$$\frac{\partial^2}{\partial y^2}(P^2) + \frac{\mu T}{K\bar{M}} \frac{\partial}{\partial y}\left(\frac{K\bar{M}}{\mu T}\right)\frac{\partial}{\partial y}(P^2) - \frac{2\mu R_u T}{K\bar{M}}\left[\frac{\partial}{\partial t}(\eta\rho) - \eta \sum_i R_{T,i} M_i\right] = 0 \tag{2}$$

The char porosity equation is

$$\frac{\partial \eta}{\partial t} = -\eta \frac{M_S}{\rho_S}\left(R_{h,s} + R_S\right) \tag{3}$$

The pyrolysis-gas temperature equation is

$$\eta \sum_i \frac{\rho_i C_{p,i}}{M_i}\left(\frac{\partial T}{\partial t} + v \frac{\partial T}{\partial y}\right) = -\eta\left(\frac{\partial \ln \rho}{\partial \ln T}\right)_{P,x_i}\left(\frac{\partial P}{\partial z} + v \frac{\partial P}{\partial y}\right) - \eta \sum_i R_{T,i} H_i + P\left(\frac{\partial \eta}{\partial t} + v \frac{\partial \eta}{\partial y}\right)$$

$$+ \frac{1}{2}\eta v^2 \sum_i R_{T,i} M_i + H_A(T_S - T) - \eta\left\{R_S\left[H(T)\right]_S\right.$$

$$\left. + R_{h,s} H_S - \sum_r r_h^{(r)} \Delta H^{(r)}\right\} \tag{4}$$

The chemical-species continuity equation is

$$\frac{\partial}{\partial t}\left(\eta\rho_i\right) + \frac{\partial}{\partial y}\left(\rho_i v_o\right) - \eta r_{T,i} = 0 \tag{5}$$

The total-mass conservation equation is

$$\frac{\partial}{\partial t}(\eta\rho) + \frac{\partial}{\partial y}\left(\rho v_o\right) - \eta \sum_i r_{T,i} = 0 \tag{6}$$

The volumetric heat-transfer coefficient for convective energy transfer from the char to the pyrolysis gases $\left(H_A \text{ in eq. (1)}\right)$ is given in reference 9 as

$$H_A = K_h \frac{v}{N_{Pr}} \eta \sum_i \frac{\rho_i C_{p,i}}{M_i} \tag{7}$$

where the proportionality constant K_h is determined experimentally.

The energy term associated with the heterogeneous chemical reactions (eqs. (1) and (4)) results from assuming that the heat of reaction for each heterogeneous reaction is supplied by the char. As an example, consider the combustion of solid carbon to form CO. The stoichiometric equation representing this reaction is

$$O_2 + 2C_s \rightarrow 2CO \tag{8}$$

The oxygen for this reaction comes from the pyrolysis gases at temperature T, the solid carbon for the reaction is at temperature T_s, and the product of the reaction (CO) is at temperature T_s. Thus the heat of reaction is

$$\Delta H = 2\left[H(T_s)\right]_{CO} - \left[H(T)\right]_{O_2} - 2\left[H(T_s)\right]_{C_s} \tag{9}$$

The chemical reaction rates appearing in equations (1) to (6) are obtained by using the following equations:

The molar rate of production of species i resulting from homogeneous chemical reactions (ref. 10) is

$$R_i = \sum_r \left[\nu_i^{(r)''} - \nu_i^{(r)'}\right] \left\{ k_f^{(r)} \prod_i \left[A_i\right]^{\nu_i^{(r)'}} - k_r^{(r)} \prod_i \left[A_i\right]^{\nu_i^{(r)''}} \right\} \tag{10}$$

The molar rate of production of species i resulting from heterogeneous chemical reactions (ref. 11) is

$$R_{h,i} = \sum_r \left[\nu_i^{(r)''} - \nu_i^{(r)'}\right] \left\{ k_f^{(r)} \prod_i \left[\theta_i\right]^{\nu_i^{(r)'}} - k_r^{(r)} \prod_i \left[\theta_i\right]^{\nu_i^{(r)''}} \right\} A_s \theta_o^{n(r)} \tag{11a}$$

where

$$n(r) = \sum_i \left[\nu_i^{(r)''} - \nu_i^{(r)'}\right] \tag{11b}$$

Equations (10) and (11) are based on the Law of Mass Action and the Law of Surface Action, respectively. They are general expressions for homogeneous and heterogeneous chemical reactions. Most frequently chemical-kinetics data for a particular reaction are obtained from empirical curve fits to experimental data. Such chemical-kinetics data are usually presented with a rate law which best describes the particular chemical process.

Uncharred-layer and substrate-insulation-layer equations.- The uncharred-layer temperature equation is

$$\frac{\partial}{\partial y}\left(k'_s \frac{\partial T'_s}{\partial y}\right) = \rho'_s \hat{C}'_{p,s} \frac{\partial T'_s}{\partial t} \tag{12}$$

The substrate-insulation-layer temperature equation is

$$\frac{\partial}{\partial y}\left(k''_s \frac{\partial T''_s}{\partial y}\right) = \rho''_s \hat{C}''_{p,s} \frac{\partial T''_s}{\partial t} \tag{13}$$

Boundary Conditions

The boundary conditions for differential equations (12) and (13) are derived for the case of stagnation heating with surface removal by oxidation in an air environment and/or sublimation and with temperature-dependent pyrolysis of the uncharred material occurring in a plane. (See ref. 8.)

Char-surface boundary conditions for solid-temperature equation.- Two conditions must be specified at the front surface of the char layer to obtain a solution to the char-layer solid-temperature equation. The first condition is an expression for either the rate of material removal or the surface temperature, and the second condition is an energy balance. When temperature and pressure conditions are such that the rate of oxygen consumption at the surface is less than the rate of diffusion of oxygen to the surface, the rate of surface removal is given by the reaction-rate equation

$$\dot{m}_c = A_s \exp\left(\frac{-B_s}{T_{s,1}}\right)\left(\frac{C_w \bar{M}_w}{M_{O_2}} P_e\right)^n \tag{14}$$

where n is the order of reaction. When the rate of oxygen consumption equals the rate of diffusion of that species to the surface, the rate of surface removal is obtained from the oxygen diffusion rate as

$$\dot{m}_c = \lambda \dot{m}_{O_2} \tag{15}$$

where λ is the ratio of the mass of char removed by oxidation to the mass of oxygen diffusing to the surface. The rate of oxygen diffusion to the surface is given by (see ref. 8)

$$\dot{m}_{O_2} = \frac{C_e - C_w}{H_e - H_w} N_{Le}^{0.6} q_{C,net} \overline{M}_w \tag{16}$$

where $q_{C,net}$ is the hot-wall convective-heating rate corrected for blocking. Thus, for diffusion-controlled oxidation

$$\dot{m}_c = \frac{C_e - C_w}{H_e - H_w} \lambda N_{Le}^{0.6} q_{C,net} \overline{M}_w \tag{17}$$

Equation (14) is combined with equation (17) to obtain an equation for the rate of surface removal by oxidation which is valid in both the rate-controlled oxidation regime and the diffusion-controlled oxidation regime. Thus, for an order of reaction of 1/2

$$\dot{m}_c = \frac{1}{2}\left\{ - \frac{(H_e - H_w)K^2 P_e}{M_{O_2} q_{C,net} \lambda N_{Le}^{0.6}} + \sqrt{\left[\frac{(H_e - H_w)K^2 P_e}{M_{O_2} q_{C,net} \lambda N_{Le}^{0.6}}\right]^2 + \frac{4K^2 C_e M_w P_e}{M_{O_2}}} \right\} \tag{18}$$

where

$$K = A_s \exp\left(\frac{-B_s}{T_{s,1}}\right) \tag{19}$$

For an order of reaction of 1

$$\dot{m}_c = \frac{K P_e C_e \overline{M}_w}{M_{O_2} + \dfrac{K P_e (H_e - H_w)}{\lambda N_{Le}^{0.6} q_{C,net}}} \tag{20}$$

Energy transfer to the surface results from convective and/or radiative heating and combustion heating caused by oxidation. This energy is accommodated by blocking due to mass injection into the boundary layer, reradiation from the surface, conduction to the interior, and sublimation of the char when the surface temperature reaches the sublimation temperature. The surface energy balance is (see ref. 4)

$$\underbrace{\underbrace{q_C}_{\substack{\text{Cold-wall}\\ \text{convective}\\ \text{heating rate}}}\underbrace{\left(1 - \frac{H_w}{H_e}\right)}_{\substack{\text{Hot-wall}\\ \text{correction}}}\underbrace{\left\{1 - (1 - \beta)\left[0.724\,\frac{H_e \dot{m}_T}{q_C \bar{M}_w} - 0.13\left(\frac{H_e}{q_C \bar{M}_w}\,\dot{m}_T\right)^2\right] - \beta\bar{\eta}\,\frac{\dot{m}_T H_e}{q_C \bar{M}_w}\right\}}_{\text{Aerodynamic blocking}}}_{\text{Net convective heating } \left(q_{C,net}\right)}$$

$$+ \underbrace{\alpha q_R}_{\substack{\text{Radiative-}\\ \text{heating rate}}} + \underbrace{\dot{m}_c \Delta H_c}_{\substack{\text{Combustion-}\\ \text{heating rate}}} = \underbrace{\sigma \epsilon_s T_{s,1}^4}_{\text{Reradiation}} - \underbrace{k_s \frac{\partial T_s}{\partial y}}_{\substack{\text{Conduction}\\ \text{to interior}}} + \underbrace{S\left(T_{s,1} - \bar{T}_1\right)\dot{m}_{sb} H_c}_{\substack{\text{Heat of sublimation}\\ \text{of char}}} \tag{21}$$

where

$$\dot{m}_T = \alpha_c \left\{S\left(T_{s,1} - \bar{T}_1\right)\left[\dot{m}_{sb} - \dot{m}_c\right] + \dot{m}_c\right\} + \alpha_p \dot{m} \tag{22}$$

and β is 1 or 0 depending on whether a first- or second-order approximation for blocking is used (ref. 4). A step function $S\left(T_{s,1} - \bar{T}_1\right)$ is defined by

$$S\left(T_{s,1} - \bar{T}_1\right) = \begin{cases} 1 & \left(T_{s,1} = \bar{T}_1\right) \\ 0 & \left(T_{s,1} < \bar{T}_1\right) \end{cases} \tag{23}$$

When the surface temperature is less than the sublimation temperature of the char material, equation (21) is used as the boundary condition for solving the char temperature equation. When the temperature of the char-layer surface equals the sublimation temperature of the char material, equation (21) is used to determine the rate of surface removal by sublimation.

Pyrolysis-zone boundary condition for solid temperature equations.- The char-layer and uncharred-layer energy equations are related through an energy balance at the pyrolysis zone; that is

$$-k_s \frac{\partial T_s}{\partial y} = \dot{m}_g \Delta H_p - k'_s \frac{\partial T'_s}{\partial y} \tag{24}$$

Also the temperatures of the two layers are equal at their interface; that is

$$T_s = T'_s \tag{25}$$

The rate of pyrolysis of the uncharred material is given by an Arrhenius type of equation

$$\dot{m}_g = A' \exp\left(\frac{-B'}{T_{s,I}}\right) \tag{26}$$

An alternative method, which allows a fixed pyrolysis temperature to be specified, is also available. When this alternative method is used, equation (24) is used to determine the interface temperature and equation (26) is used to determine the pyrolysis rate until the pyrolysis temperature reaches the specified value. Then equation (24) is used to determine the rate of pyrolysis and the interface temperature is given by

$$T_{s,I} = \bar{T}_I \tag{27}$$

Uncharred-layer—insulation-layer interface boundary condition.- The boundary condition at the uncharred-layer—insulation-layer interface is

$$-k'_s \frac{\partial T'_s}{\partial y} = -k''_s \frac{\partial T''_s}{\partial y} + \rho_{HS} \hat{C}_{p,HS} l_{HS} \frac{\partial T'_s}{\partial t} \tag{28}$$

The temperature of the two layers is also equal at their interface; that is

$$T'_s = T''_s \tag{29}$$

Back-surface boundary condition for solid temperature equation.- The energy transferred to the back surface (conduction through the insulation plus energy transfer to the back surface from the surroundings) is accommodated by reradiation to the surroundings and by an increase in the temperature of the heat sink at the back surface. The boundary condition is

$$-k''_s \frac{\partial T''_s}{\partial y} + q_B = \sigma \epsilon''_s \left(T''_s\right)^4 + \rho_{HSP} \hat{C}_{p,HSP} l_{HSP} \frac{\partial T''_s}{\partial t} \tag{30}$$

where q_B is the net heat-transfer rate from the surroundings to the back surface. The effect of an adiabatic back surface is achieved by setting q_B equal to the rate of energy radiated by the surface to the surroundings. Thus, for an adiabatic back surface

$$q_B = \sigma \epsilon''_s \left(T''_s\right)^4 \tag{31}$$

Boundary conditions for pyrolysis-gas pressure equation.- The differential equation for pyrolysis-gas pressure requires two boundary conditions. The first boundary condition is that the pressure be specified at the char surface; that is

$$P = P_w \tag{32}$$

The second boundary condition is that the pressure gradient at the pyrolysis zone be proportional to the pyrolysis rate. Darcy's equation for one-dimensional fluid velocity in a porous medium is (ref. 12)

$$v_o = -\frac{K}{\mu} \frac{\partial P}{\partial y} \tag{33}$$

By multiplying by the fluid density and by using the equation of state, the following equation is obtained

$$\rho v_o = -\frac{K\bar{M}}{\mu R_u T} P \frac{\partial P}{\partial y} \tag{34}$$

At the pyrolysis zone

$$\rho v_o = -\dot{m}_g \tag{35}$$

Therefore, at the pyrolysis zone

$$\frac{\partial}{\partial y}(P^2) = 2R_u \frac{\mu T}{K\bar{M}} \dot{m}_g \tag{36}$$

Boundary condition for char porosity equation.- A single boundary condition is required for solution of the char porosity equation. The condition used in this analysis is that of a specified porosity of the char layer at the pyrolysis zone.

Boundary condition for pyrolysis-gas temperature equation.- The pyrolysis-gas temperature boundary condition used is that the pyrolysis-gas temperature be equal to the solid temperature at the pyrolysis zone.

Boundary condition for total-mass conservation equation.- The mass-conservation-equation boundary condition used is that the mass-flow rate be known at the pyrolysis zone; that is

$$\rho v_o = -\dot{m}_g \tag{37}$$

Boundary condition for chemical-species conservation equation.- The chemical-species conservation-equation boundary condition is obtained from the molar composition of the pyrolysis gases, which is specified at the pyrolysis zone, and the total-mass-flow rate at that point. This boundary condition is

$$\rho_i v = -\frac{x_i M_i}{\eta \bar{M}} \dot{m}_g \tag{38}$$

Initial Conditions

The initial conditions of all parameters necessary to describe the thermochemical state of an ablation system are specified. These conditions may be other than zero and the spacial parameters may have initial values which vary with location.

Coordinate Transformation

The governing equations presented here are partial differential equations with variable coefficients. Thus, they must be solved numerically. These equations are transformed to dimensionless coordinate systems attached to the ablator boundaries (see fig. 1) to eliminate the problem of error accumulation associated with numerical solutions in fixed coordinate systems for layers which vary in thickness with time. Details of the coordinate transformation are given in appendix A.

Solution of Equations

All differential equations and boundary conditions presented in the previous sections except the total-mass conservation equation are written in modified implicit finite-difference form so that they may be solved by using a digital computer. The finite-

difference equations are formulated in appendix B. Figure 2 shows the location of the finite-difference stations.

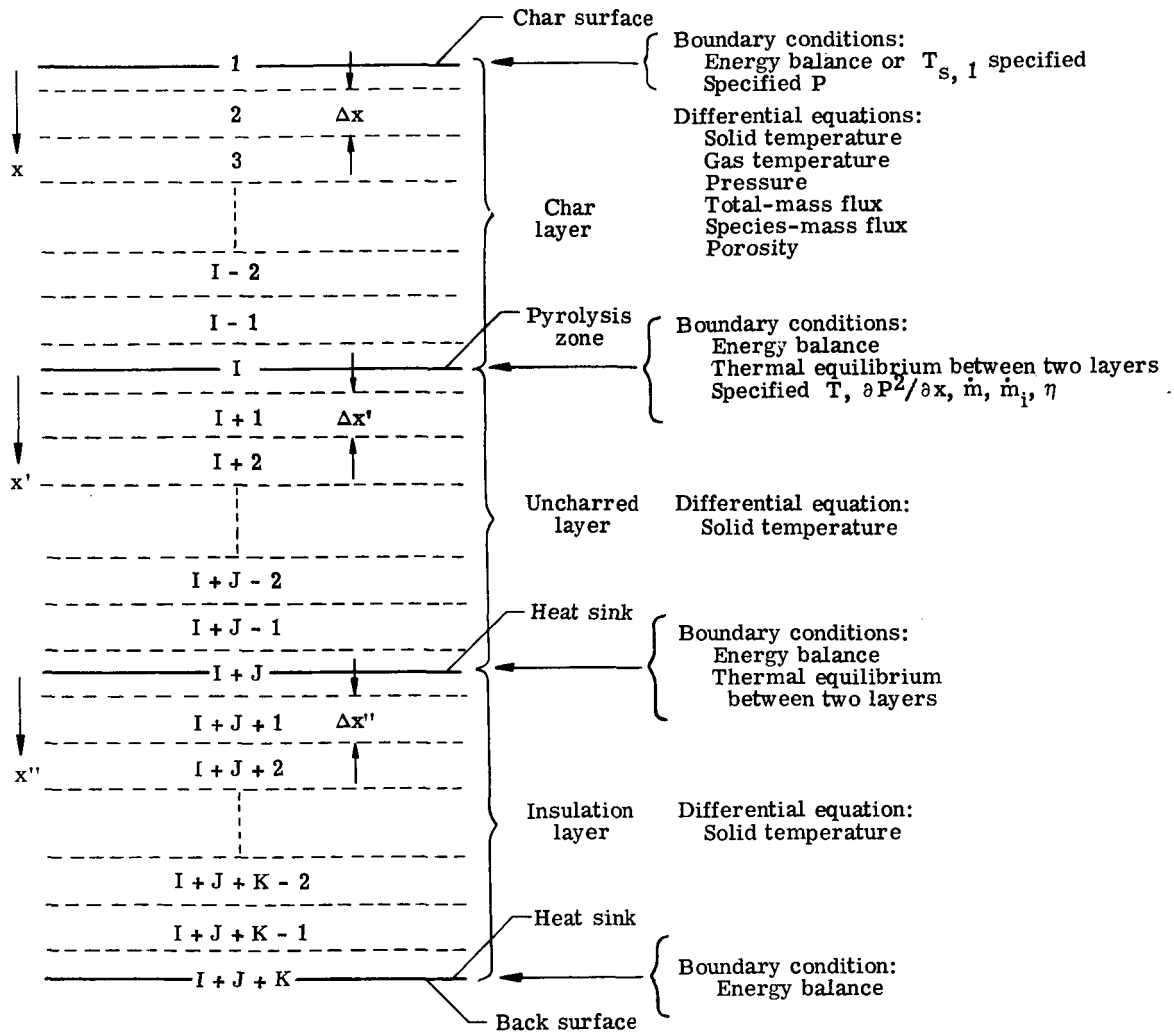

Figure 2.- Location of finite-difference stations.

The sets of finite-difference equations obtained from the second-order differential equations are tridiagonal and are

$$\left.\begin{aligned} &B(1)\ \phi(1) + C(1)\ \phi(2) = D(1) \\ &A(N)\ \phi(N-1) + B(N)\ \phi(N) + C(N)\ \phi(N+1) = D(N) \qquad (1 < N < K) \\ &A(I)\ \phi(I-1) + B(I)\ \phi(I) = D(I) \end{aligned}\right\} \tag{39}$$

where the boundary equations have been reduced to the standard tridiagonal form by combining them with the equations for neighboring stations. The sets of finite-difference equations obtained from the first-order differential equations are not symmetric with respect to the diagonal elements. These equations are

$$\left.\begin{aligned} &B(N)\ \theta(N) + C(N)\ \theta(N+1) + E(N)\ \theta(N+2) = D(N) \qquad (1 \leq N < I-1) \\ &B(I-1)\ \theta(I-1) + C(I-1)\ \theta(I) = D(I-1) \end{aligned}\right\} \tag{40}$$

These sets of equations are solved by a method which is equivalent to Gaussian elimination (ref. 13).

The transformed-mass conservation equation is written in integral form as

$$\dot{m}(N) = \dot{m}_g - \ell \int_{x(N)}^{x(I)} \left\{ \frac{\partial}{\partial t}(\eta\rho) - \eta \sum_i R_{T,i} M_i \frac{1}{\ell} \left[\frac{\dot{m}_s}{\rho_{s,0}} + x\left(\frac{\dot{m}_g}{\Delta\rho} - \frac{\dot{m}_s}{\rho_{s,0}} \right) \right] \frac{\partial}{\partial x}(\eta\rho) \right\} dx \tag{41a}$$

where

$$\dot{m}_s = \left[1 - S\left(T_{s,1} - \bar{T}_1 \right) \right] \dot{m}_c + S\left(T_{s,1} - \bar{T}_1 \right) \dot{m}_{sb} \tag{41b}$$

and the integral is evaluated numerically from station N to the pyrolysis zone (station I).

RESULTS AND DISCUSSION

The accuracy of various parts of the numerical analysis is verified by comparing the numerical results with exact solutions for a number of simplified problems. The derivation of the exact solutions are given in appendix C. Some typical results are also given for a charring ablator subjected to a constant heating rate. These results are discussed in the following sections.

Comparison of Numerical Results With Exact Solutions

The equations governing the transient response of an ablation system are too complex to solve exactly for the general case. However, exact solutions for a number of simplified problems serve as a check of results obtained by using the finite-difference equations.

The exact solutions employed herein are for the following problems:

(1) The pressure distribution for a constant property, incompressible, isothermal fluid flowing through an isothermal slab

(2) The transient temperature response of a constant property, incompressible fluid flowing through an isothermal slab

(3) The transient temperature response of a heat sink subjected to a suddenly applied constant heating rate

(4) Quasi-steady-state ablation

Pressure distribution for constant property, incompressible, isothermal fluid flowing through an isothermal slab.- Table 1 shows errors in pressure solutions for flow of a constant property, incompressible, isothermal fluid through an isothermal slab. The exact solution was obtained by using equation (C5), and the numerical solution was obtained by using the finite-difference equation of this analysis. Note that the error is much less than 0.004 percent throughout the thickness of the slab.

TABLE 1.- ERRORS IN NUMERICAL AND EXACT SOLUTIONS FOR PRESSURE DISTRIBUTION IN A CHAR LAYER FOR A SIMPLIFIED MODEL

[Input values used were: $\ell = 0.01$ m; $K = 2 \times 10^{-10}$ m^2; $T = 750$ K; $\dot{m}_g = 0.05$ kg/m^2-sec; $\mu = 2.75 \times 10^{-5}$ N-sec/m^2; and $\overline{M} = 0.02895$ kg/g-mol]

x	Percent error[a] in P for –	
	$P_w = 0.01$ atm[b]	$P_w = 0.1$ atm[b]
0	-------	--------
1/4	0.00285	0.000215
1/2	.00308	.000406
3/4	.00311	.000571
1	.00319	.000726

[a] Percent error $= \dfrac{P_{exact} - P_{calculated}}{P_{exact}} \times 100.$

[b] 1 atm $= 1.013 \times 10^5$ N/m^2.

Transient temperature response of constant property, incompressible fluid flowing through an isothermal slab.- The exact solution for flow of a constant property, incompressible fluid through an isothermal slab is given by equations (C13). Figures 3 and 4

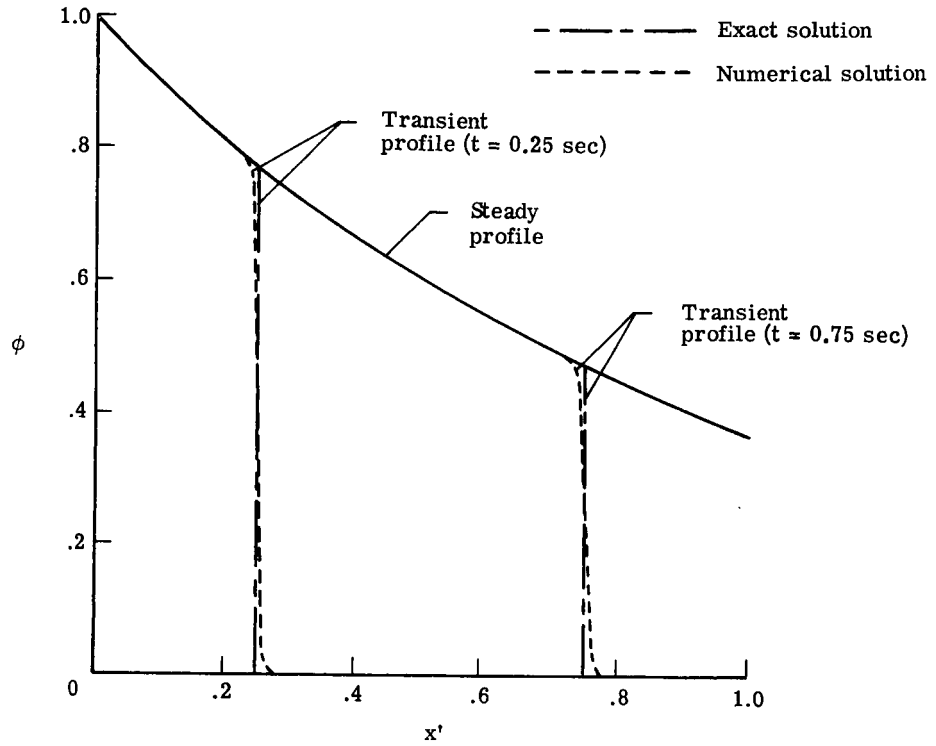

Figure 3.- Numerical and exact temperature solutions for flow of a constant property, incompressible fluid through an isothermal slab with $\Delta x = 0.001$.

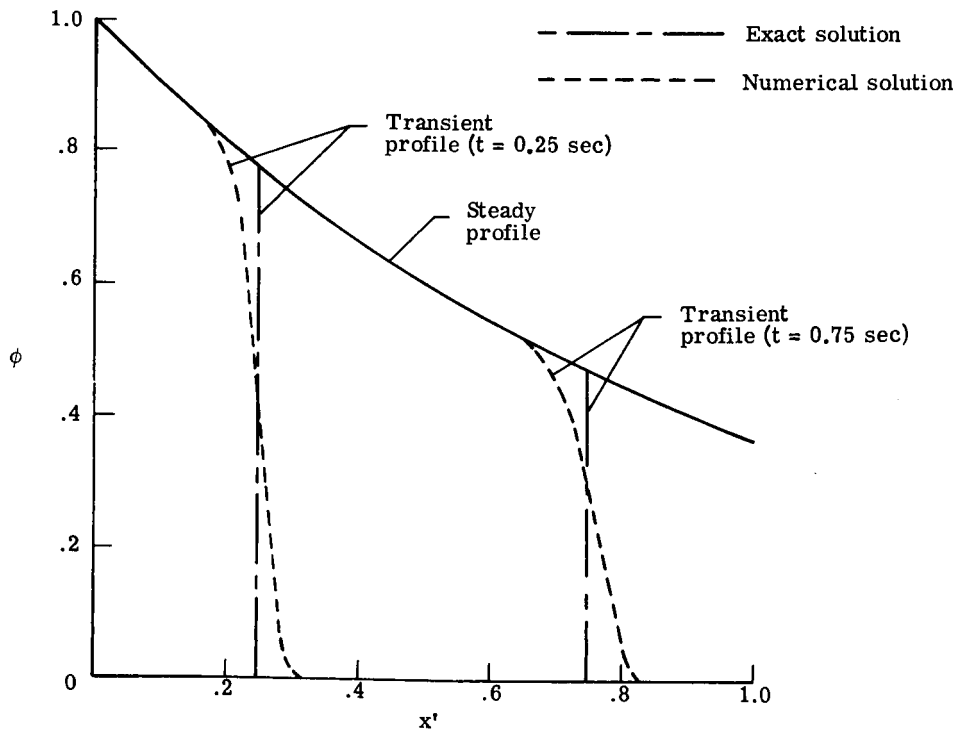

Figure 4.- Numerical and exact temperature solutions for flow of a constant property, incompressible fluid through an isothermal slab with $\Delta x = 0.01$.

show comparisons of results obtained by using this equation and results obtained by using the finite-difference equations with difference spacings of 0.001 and 0.01, respectively. The comparison with the transient results is favorable for the fine spacing, but as expected, the accuracy is poorer for the larger grid spacing. The steady profile solutions differ less than 0.02 percent for each case.

Transient temperature response of a heat sink subjected to a suddenly applied constant heating rate.- The exact solution for the temperature response of a flat plate subjected to a suddenly applied constant heating rate is given by equation (C14). This equation was used with the heating rate and material properties listed in table 2 to determine the transient response of a flat plate. Solutions were obtained for the same problem by using the finite-difference equations.

TABLE 2.- INPUTS USED IN HEAT-SINK EXACT SOLUTION

q, W/m^2	1×10^4
l, m	0.01
l', m	0.01
k_s, W/m^2-K	0.624
ρ_s, kg/m^3	2140
$\hat{C}_{p,s}$, J/kg-K	715.16
$T_{s,o}$, K	300

Figure 5 shows the numerical solutions for time steps of 0.01 and 0.1 second and the exact solution. Even for the large time step of 0.1 second, the error at $t = 1.0$ second is less than 3 percent.

Quasi-steady-state ablation.- In quasi-steady-state ablation, the pyrolysis interface and the front surface recede at the same rate; that is, the char thickness is constant. If, in addition, the pyrolysis gases are inert, incompressible, and in local thermal equilibrium with the char layer; properties of the system are uniform and independent of temperature; there are no energy sources, viscous dissipation, or diffusion; and conditions exist such that no energy is transferred into the uncharred layer; then the exact solution to the governing equations is given by equations (C27).

Numerical solutions were obtained by using the finite-difference equations with the data contained in table 3. The assumption of incompressibility was satisfied by specifying a constant pyrolysis-gas density. To satisfy the assumption of local thermal equilibrium between the pyrolysis gases and the char layer, a very large value was used for the

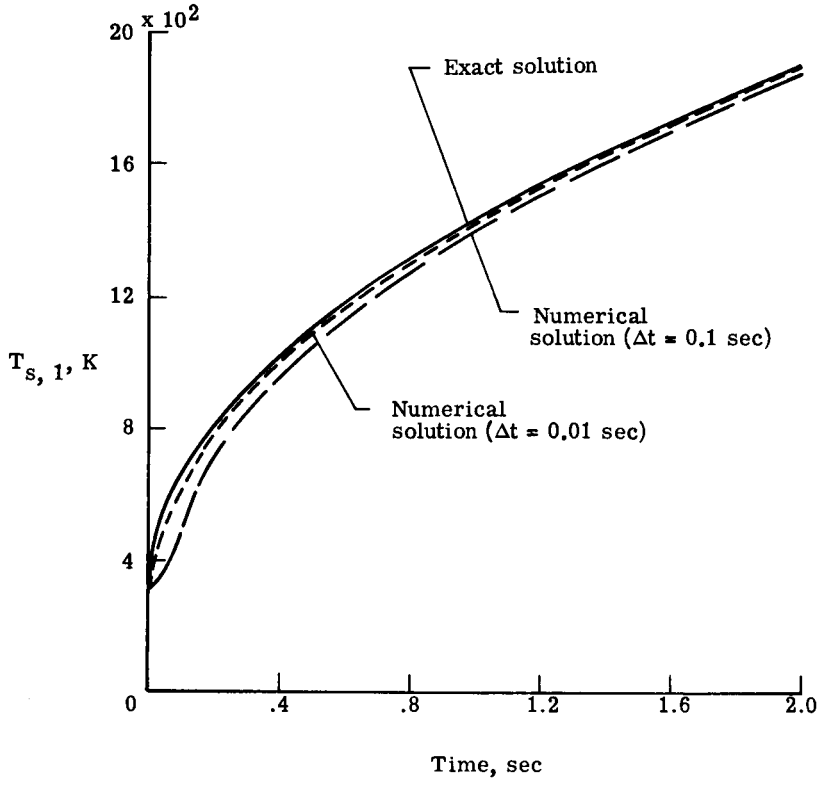

Figure 5.- Numerical results and exact solutions for heat-sink problem.

TABLE 3.- INPUTS USED IN QUASI-STEADY-STATE ABLATION EXACT SOLUTION

q_{AERO}, W/m^2	8×10^5
k_s, W/m-K	0.624
$\rho_{s,0}$, kg/m^3	320
$\Delta\rho$, kg/m^3	320
$\hat{C}_{p,s}$, J/kg-K	2090
$\hat{C}_p$, J/kg-K	2090
$\bar{T}_1$, K	2222
$\bar{T}_I$, K	556
ΔH_p, J/kg	2.324×10^6
H_c, J/kg	2.324×10^6
$\bar{M}$, kg/g-mol	0.029

proportionality constant appearing in the equation for H_A, the convective-heat-transfer coefficient; that is

$$H_A = \frac{K_h v \eta}{N_{Pr}} \sum_i \frac{\rho_i C_{p,i}}{M_i} \tag{42}$$

Calculations made by using a value for K_h of 5×10^5 1/m indicated a temperature difference of only 1.5 K between the char layer and the pyrolysis gases at the front surface. The results from this calculation are compared with the exact solution in table 4. The calculated char thickness and mass-loss rates are within 2 percent of the exact solution.

TABLE 4.- EXACT SOLUTION AND NUMERICAL SOLUTION OBTAINED WITH $K_h = 5 \times 10^5$ 1/m FOR QUASI-STEADY-STATE ABLATION

Parameter	Unit	Numerical solution	Exact solution	Percent error
$\dot{m}_s$	kg/m^2-sec	7.304×10^{-2}	7.185×10^{-2}	1.66
$\dot{m}_g$	kg/m^2-sec	7.301×10^{-2}	7.185×10^{-2}	1.61
l	m	2.924×10^{-3}	2.973×10^{-3}	-1.65

An additional set of calculations was made in which the pyrolysis-gas temperature was set equal to the char-layer temperature and the term $H_A(T_s - T)$ appearing in the char-layer equation was replaced by the expression

$$\frac{1}{l}\left(\dot{m}_g - \eta\rho \frac{\dot{m}_s}{\rho_{s,0}}\right)\left(\hat{C}_p - \frac{R_u}{\bar{M}}\right)\frac{\partial T_s}{\partial x} \tag{43}$$

which satisfied the assumption of local thermal equilibrium between the pyrolysis gases and the char layer. Results from this calculation are shown in figure 6 and are within 1 percent of the exact solution after quasi-steady state is obtained. Note that the system reached a quasi-steady-state condition after only 25 seconds. The near discontinuity in the surface-removal-rate curve illustrates the three regimes of mass removal at the surface. The initial segment of the curve represents that portion of time when oxidation of the char layer was reaction-rate controlled. The second portion of lesser slope represents the time period when the rate of oxidation of the char layer was governed by the rate of diffusion of oxygen through the boundary layer. The final portion of the curve represents the time during which the char layer was subliming.

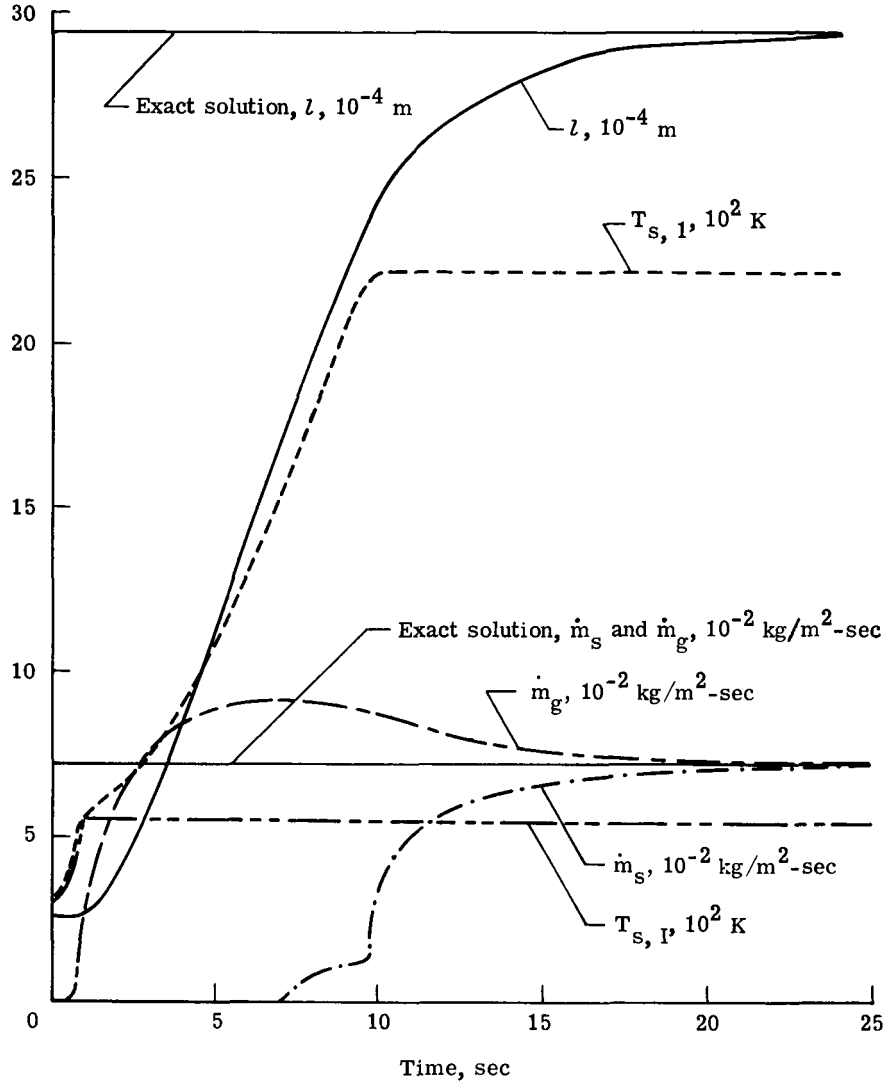

Figure 6.- Numerical results for $\dot{m}_s$, $\dot{m}_g$, l, $T_{s,1}$, and $T_{s,I}$ for a case run to quasi-steady-state ablation condition.

Numerical Results for an Ablation System Experiencing Thermal, Chemical, and Mass-Transfer Processes

Figures 7 and 8 present numerical solutions for a charring ablator system subjected to a constant heating rate. The ablator system considered here is typical of the general ablation problem in that thermal nonequilibrium of the char layer and pyrolysis gases exists and chemical reactions with mass deposition occur within the char layer. The heating rate, enthalpy, and pressure histories used in this calculation are given in table 5, and the material properties used are given in table 6 (from ref. 14). Table 7 lists the chemical reactions and kinetics data. Figure 7 shows time histories of surface removal, pyrolysis rate, char thickness, char-surface temperature, and pyrolysis-gas temperature

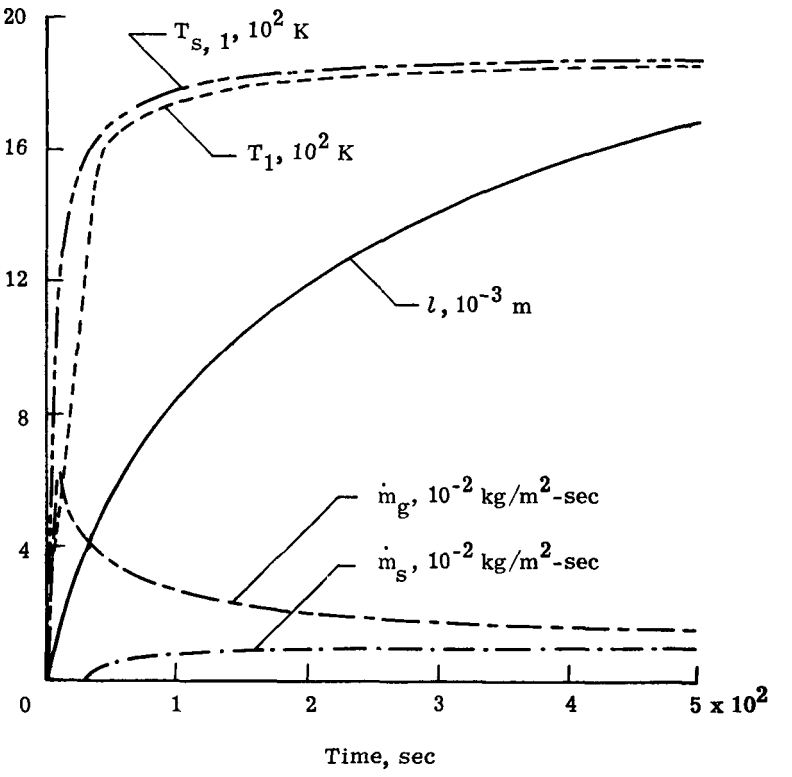

Figure 7.- Typical time histories of $\dot{m}_s$, $\dot{m}_g$, l, surface temperature, and pyrolysis-gas temperature at surface for an ablation system subjected to constant heating rate.

TABLE 5.- TRAJECTORY DATA USED IN MAKING CALCULATIONS FOR AN ABLATION SYSTEM WITH THERMAL, CHEMICAL, AND MASS TRANSFER

q_C, W/m^2, at time, sec:	
0	2.162×10^3
10	8.0×10^5
1000	8.0×10^5
P_W, N/m^2, at time, sec:	
0	1.0×10^{-6}
9	1.0×10^{-4}
29	9.0×10^{-4}
39	1.0×10^{-1}
1000	1.0×10^{-1}
H_e, J/kg	3.1×10^5
C_e	0.23

at the surface. These parameters change very rapidly at early times, but after 100 seconds the temperature and mass-transfer rates are approaching steady state. The spike in $\dot{m}_g$ at 10 seconds corresponds to the rapid increase in system temperature at initiation of heating. The sharp drop in $\dot{m}_g$ results from the growth of the char layer which insulates the pyrolysis zone and from the blocking effect of the pyrolysis gases which reduces the heat transfer to the char surface. The initial steep slope of the surface mass-loss curve $\dot{m}_s$ is associated with the rate-controlled (highly temperature-dependent) oxidation regime. The curve for $\dot{m}_s$ undergoes an orderly transition to the much flatter region which corresponds to the diffusion-controlled oxidation regime.

Figure 8 shows profiles of pyrolysis-gas temperature, molecular weight, mass-flow rate, pressure, char-layer temperature and porosity at a time of 500 seconds for the same case. Note that $x = 0$ is the char-layer surface and $x = 1$ is the pyrolysis zone. The presence of chemical reactions and mass deposition is indicated by the decrease in molecular weight and pyrolysis-gas mass-flow rate.

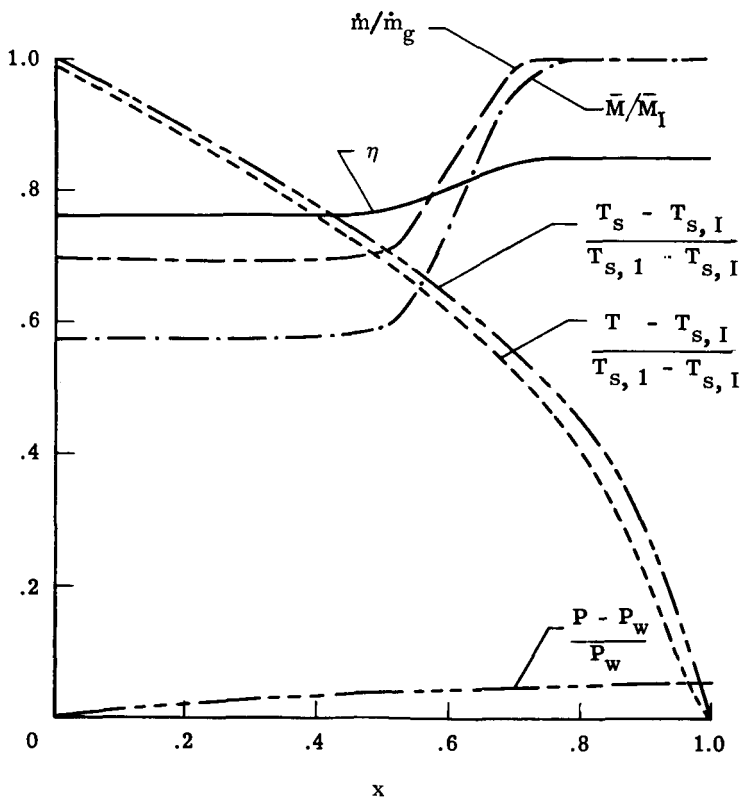

Figure 8.- Profiles of pyrolysis-gas temperature, char-layer temperature, pyrolysis-gas molecular weight, char porosity, local mass-flow rate, and pyrolysis-gas pressure at time of 500 sec. (See fig. 7.) Char thickness = 1.646×10^{-2} m; $P_w = 1.013 \times 10^4$ N/m^2; $\dot{m}_g = 1.52 \times 10^{-2}$ kg/m^2-sec; $\bar{M}_I = 2.573 \times 10^{-2}$ kg/g-mol; $T_{s,1} - T_{s,I} = 1312$ K.

TABLE 6.- THERMOPHYSICAL PROPERTIES OF LOW-DENSITY PHENOLIC-NYLON ABLATION MATERIAL (REF. 14)

Char:	
Oxidation kinetics (first order):	
Specific reaction rate constant, kg/m^2-sec-atm	4.90×10^{10}
Activation energy, K	4.25×10^4
Mass of char removed per mass of oxygen reaching surface	0.75
Heat of combustion, J/kg	1.20×10^7
Heat of sublimation, J/kg	5.00×10^7
Surface emissivity	0.80
Theoretical density, kg/m^3	1.43×10^3
Porosity at pyrolysis zone	0.85
Proportionality constant in equation for gas char heat-transfer coefficient, 1/m	1.00×10^3
Permeability, m^2	1.00×10^{-9}
Thermal conductivity, W/m-K, at temperature of –	
278 K	0.16
833 K	0.16
1110 K	0.50
1390 K	1.22
1670 K	1.87
1940 K	2.65
2220 K	3.74
2500 K	4.75
2780 K	6.24
3050 K	7.66
Uncharred material:	
Density, kg/m^3	5.53×10^2
Pyrolysis kinetics:	
Specific reaction rate constant, kg/m^2-sec-atm	7.74×10^6
Activation energy, K	1.289×10^4
Effective heat of pyrolysis, J/kg	1.28×10^6
Specific heat, J/kg-K, at temperature of –	
311 K	1.51×10^3
367 K	1.80×10^3
423 K	2.07×10^3
478 K	2.24×10^3
533 K	2.28×10^3
589 K	2.28×10^3
Thermal conductivity, W/m-K, at temperature of –	
300 K	0.080
390 K	0.084
500 K	0.088
610 K	0.092
710 K	0.094
Initial composition of pyrolysis gases, mole fraction of chemical species at pyrolysis zone:	
CH_4	0
H_2	0.294
C_2H_4	0
C_2H_2	0
CO	0.59
H_2O	0
NH_3	0
N_2	0.009
CO_2	0
HCN	0
C_2H_6	0
C_6H_6	0.107

TABLE 7.- CHEMICAL REACTIONS INVOLVING PYROLYSIS GASES AND CHAR

General reaction: $aA + bB + \ldots \underset{k_r}{\overset{k_f}{\rightleftharpoons}} nN + oO + \ldots$ where $k = A \exp(-B/T)$

Reaction	Type	Rate law	Frequency factor, A	Activation energy, B, K
$CH_4 \rightarrow \frac{1}{2} C_2H_6 + \frac{1}{2} H_2$	Homogeneous	k_fA	7.60×10^{14}	4.775×10^4
$C_2H_6 \rightarrow C_2H_4 + H_2$	Homogeneous	k_fA	3.14×10^{15}	3.019×10^4
$C_2H_4 \rightarrow C_2H_2 + H_2$	Homogeneous	k_fA	2.57×10^8	1.157×10^5
$C_2H_2 \rightarrow 2C + H_2$	Homogeneous	k_fA^2	2.14×10^{10}	2.009×10^4
$C_6H_6 \rightarrow 6C + 3H_2$	Homogeneous	k_fA	1.40×10^{11}	2.622×10^4
$C + CO_2 \rightarrow 2CO$	Heterogeneous	k_fB	1.20×10^{12}	4.282×10^4
$C + H_2O \rightarrow CO + H_2$	Heterogeneous	k_fB	9.26×10^3	3.524×10^4
$NH_3 \rightarrow \frac{1}{2} N_2 + 1\frac{1}{2} H_2$	Homogeneous	k_fA	2.86×10^6	3.055×10^4
$NH_3 + C \rightarrow HCN + H_2$	Heterogeneous	k_fA	8.78×10^6	3.885×10^4

Figures 7 and 8 demonstrate the capability of this analysis to obtain solutions for the general ablation problem. The significance of this capability lies in the increased accuracy of the results and the greater detail in which the thermal, chemical, and mass-transfer processes are treated compared with previous treatments of the problem. The governing mass-transfer equations are solved numerically in their fully transient form compared with the previously used quasi-steady form.

The detail in which the chemical and mass-transfer processes are treated provides a complete characterization of the pyrolysis gases injected into the boundary layer and describes the char-layer densification by mass deposition. The complete characterization of the pyrolysis gases leaving the char layer is critical in making calculations for the flow field about an ablating body since the injected species strongly influence the flow-field chemistry. Consideration of mass deposition in the char layer results in a more accurate calculation of char density. The surface recession rate is directly related to the char-layer density at the surface; thus an accurate description of the mass-deposition processes enables a more accurate computation of the total-surface recession.

The full significance of possessing the capability of treating thermal nonequilibrium of the char layer and pyrolysis gases is not known at this time because the fluid-solid

heat-transfer characteristics of charring ablators have not been determined. Any lag of the pyrolysis-gas temperature relative to the char temperature usually reduces the benefits obtained from thermal, chemical, and mass-transfer processes in the char layer compared with the case with thermal equilibrium between the two phases.

The effects of the fluid-solid heat-transfer characteristics on charring-ablator thermal performance are shown in figure 9. Profiles were calculated for ablation materials of the same thickness (but different fluid-solid heat-transfer characteristics) exposed to a constant-heating-rate environment until all the material was pyrolyzed. The abscissa in figure 9 is the constant K_h in equation (7) which defines the fluid-solid heat-transfer coefficient of the porous char layer. The pyrolysis-gas—char-layer temperature difference at the char surface is a measure of the thermal nonequilibrium of the system, and the exposure time required for pyrolysis of a given thickness of material is a measure of the thermal performance of the material. The molecular weight of the pyrolysis gases leaving the char layer indicates the extent of the chemical reactions occurring in the char layer.

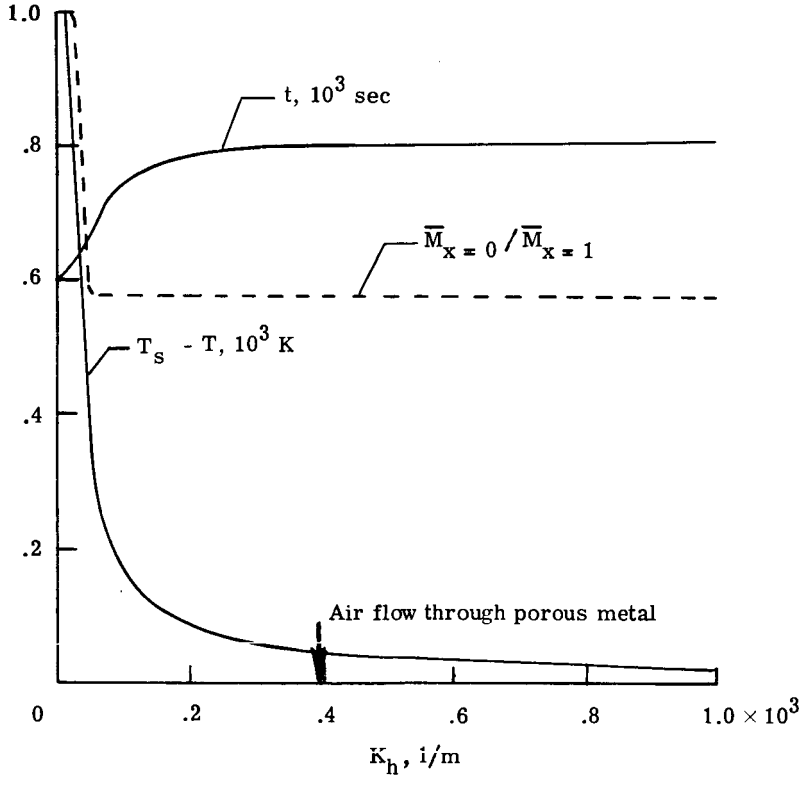

Figure 9.- Effect of pyrolysis-gas—char-layer heat-transfer characteristics on performance of ablators. $q = H_A(T_s - T)$; $H_A = \frac{K_h \eta v}{N_{Pr}} \sum_i \frac{\rho_i C_{p,i}}{M_i}$.

As a point of reference for figure 9, K_h for air flow through porous metal with a porosity of 0.4 is about 400 per meter (ref. 9). At values of K_h of 400 and larger the pyrolysis-gas—char-layer temperature difference is less than 50 K and the time to complete pyrolysis is within 2 percent of the limiting value obtained when $T = T_s$. At values of K_h less than 200 the pyrolysis-gas—char-layer temperature difference is much larger and the time to complete pyrolysis approaches its lower limit which is 75 percent of its upper limit.

In figure 9 a very sharp transition in pyrolysis-gas molecular weight occurs around $K_h = 40$ per meter. At values of K_h greater than 50 per meter the chemical species injected into the boundary layer are in equilibrium; however, the location within the char layer at which the chemical reactions occur is affected. Figure 10 shows profiles of pyrolysis-gas molecular weight in the char layer for several values of K_h ranging from 50 per meter to 1000 per meter. This figure shows that a larger K_h results in chemical reactions occurring nearer the pyrolysis zone where heat absorption processes are more effective.

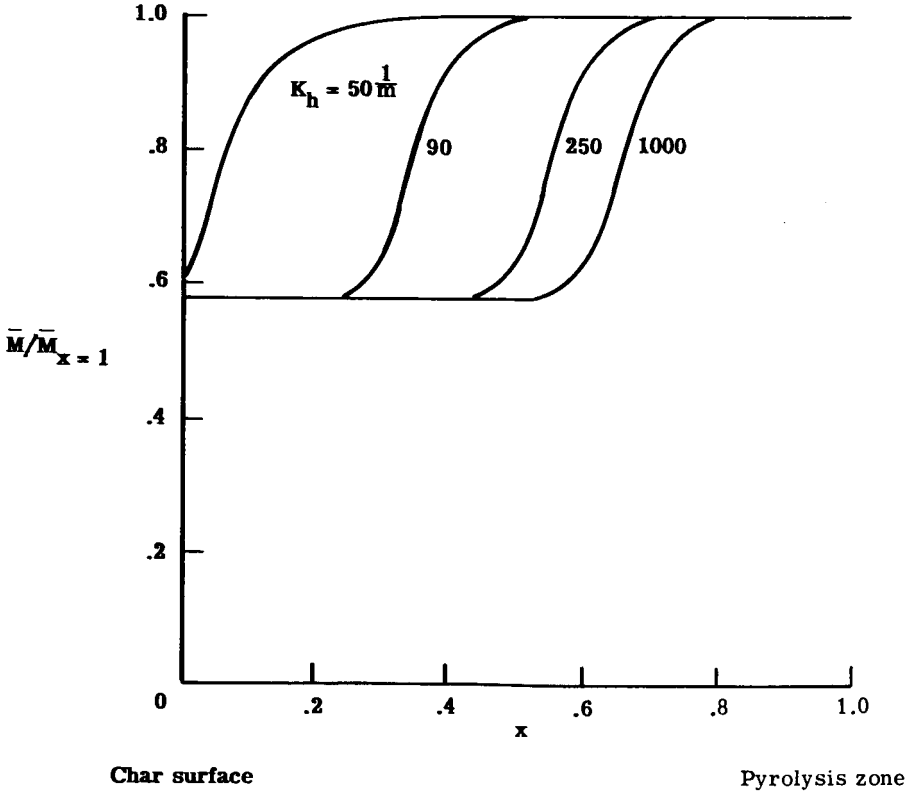

Figure 10.- Effect of pyrolysis-gas—char-layer heat-transfer characteristics on chemical processes in ablators.

Comparison of Current Results With Those From Previous Analyses

Calculations were made by using this analysis and the analysis of reference 4 for an ablator system subjected to a constant heating rate. In each case calculations were made for constant heating until all the uncharred material was pyrolyzed. Results from these calculations are shown in figures 11 and 12. Figure 11 shows histories of char- and uncharred-layer thicknesses and surface temperature. Figure 12 shows the surface-removal rates and the pyrolysis rates.

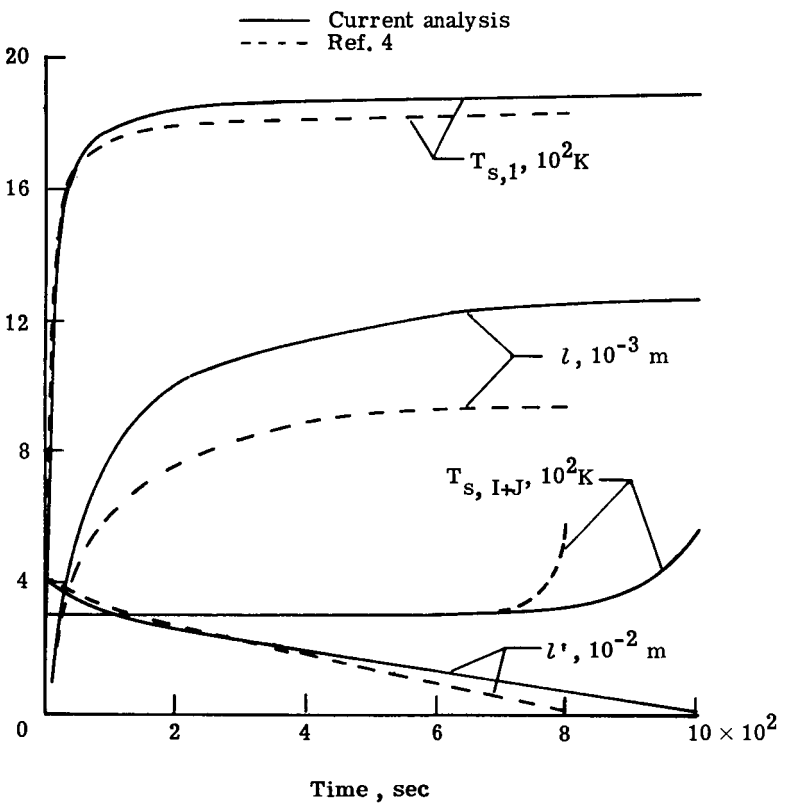

Figure 11.- Thickness and temperature histories obtained with current analysis and reference 4 for an ablator subjected to constant heating.

The current analysis indicates that the time to experience a back-surface temperature rise of 167 K is 16 percent greater than the time indicated by the analysis of reference 4 (fig. 11). This difference in time results from the mass deposition in the char layer which is treated in this analysis but neglected in reference 4. Mass deposition densifies the char layer near the front surface and results in a thicker char layer as shown in figure 11. The thicker char layer provides greater insulation of the pyrolysis zone and, hence, a lower pyrolysis rate as shown in figure 12. The lower pyrolysis rate provides less convective blocking at the front surface, thereby, resulting in a slightly higher surface temperature (see fig. 11) and surface removal rate (see fig. 12).

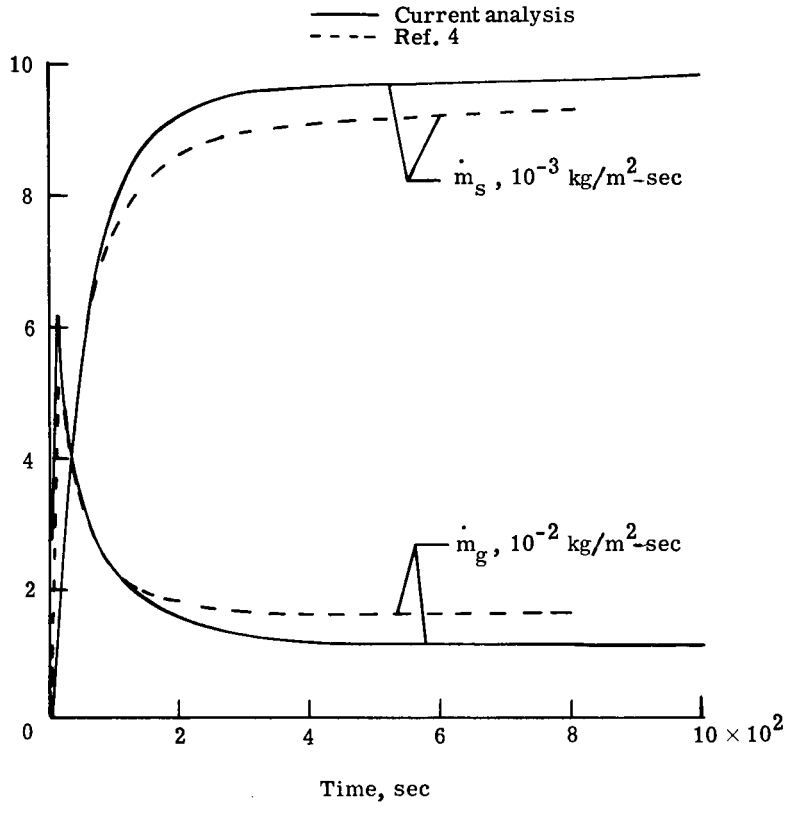

Figure 12.- Mass-transfer histories obtained with current analysis and reference 4 for an ablator subjected to constant heating.

The presence of deposition in the char layer of ablators has been known for some time. Ablation calculations have been made in the past by using the analysis of reference 4 wherein modifications of the input data were included to account for the presence of char-layer deposition. The difference in the results obtained with these two analyses is caused by a process which has been handled effectively by empirical means prior to this time. The present analysis provides a quantitative theory to calculate gas-phase reaction effects such as carbon deposition. Therefore, the present analysis can not only be used to validate results obtained with simplified analysis; but it also provides guidance in modifying the simplified analyses to include gas-phase reactions with engineering accuracy.

CONCLUDING REMARKS

A one-dimensional analysis of the transient response of an ablative thermal protection system, including a detailed treatment of the various thermal, chemical, and mass-transfer processes, is presented. These equations are solved numerically by using a modified implicit finite-difference scheme. Numerical results compare favorably with exact solutions for a number of simplified cases.

Calculated results for an ablative material subjected to a constant moderate heating rate show that thermal nonequilibrium, chemical effects, and the overall performance of charring ablators are strongly affected by the pyrolysis-gas—char-layer heat-transfer characteristics. For the condition analyzed, as the gas-char heat-transfer coefficient is reduced below about one-half the value for air flow through porous metal, the pyrolysis-gas—char-layer temperature difference becomes significant and the total performance drops sharply. The pyrolysis gases leaving the char layer have undergone degradation to their low-molecular weight form except at very low values of gas-char heat-transfer coefficient.

Calculations made with this analysis show that ablator performance is 16 percent better than is indicated by calculations with a less detailed treatment of the thermal, chemical, and mass-transfer processes. This difference results primarily from consideration of mass deposition in the char layer.

Langley Research Center,
National Aeronautics and Space Administration,
Hampton, Va., March 19, 1973.

APPENDIX A

TRANSFORMATION OF COORDINATES

The transformation of the governing equations from the fixed coordinate system to the moving coordinate systems attached to the ablator boundaries (see fig. 1) is presented in this appendix.

Location of System Boundaries

The char surface moves with respect to a fixed coordinate system when surface removal occurs. The change in location of this boundary with respect to time is given by

$$\bar{y} = \int_0^t \frac{\dot{m}_s}{\rho_{s,0}}\, dt \tag{A1a}$$

where

$$\dot{m}_s = S\left(T_{s,1} - \bar{T}_1\right)\dot{m}_{sb} + \left[1 - S\left(T_{s,1} - \bar{T}_1\right)\right]\dot{m}_c \tag{A1b}$$

and the change in location of the pyrolysis zone with respect to time is

$$\bar{y}' = \int_0^t \frac{\dot{m}_g}{\Delta\rho}\, dt \tag{A2}$$

The char-layer thickness at any time t is given by

$$l = l_0 + \int_0^t \left(\frac{\dot{m}_g}{\Delta\rho} - \frac{\dot{m}_s}{\rho_{s,0}}\right) dt \tag{A3}$$

and the uncharred-layer thickness at any time t is given by

$$l' = l'_0 - \int_0^t \frac{\dot{m}_g}{\Delta\rho}\, dt \tag{A4}$$

Coordinate Transformations

The equations and boundary conditions for the char layer are transformed to a nondimensional moving coordinate system with $x = 0$ at the front surface and $x = 1$ at the pyrolysis zone by using the following transformation (see ref. 4)

$$x = \frac{y - \int_0^t \frac{\dot{m}_s}{\rho_{s,0}}\,dt}{l} \tag{A5}$$

Similarly, the governing equations and boundary conditions for the uncharred layer are transformed to a nondimensional moving coordinate system with $x' = 0$ at the pyrolysis zone and $x' = 1$ at the uncharred-layer—insulation-layer interface by using the following transformation (ref. 4)

$$x' = \frac{y - l_o - \int_0^t \frac{\dot{m}_g}{\Delta\rho}\,dt}{l'} \tag{A6}$$

The boundaries of the insulation layer are also nondimensionalized with the transformation

$$x'' = \frac{y - \left(l_o + l'_o\right)}{l''} \tag{A7}$$

By using these equations, the space derivatives in the fixed coordinate system become: For the char layer

$$\left.\begin{aligned} \frac{\partial}{\partial y} &= \frac{1}{l}\frac{\partial}{\partial x} \\ \frac{\partial^2}{\partial y^2} &= \frac{1}{l^2}\frac{\partial^2}{\partial x^2} \end{aligned}\right\} \tag{A8}$$

For the uncharred layer

$$\left.\begin{aligned} \frac{\partial}{\partial y} &= \frac{1}{l'}\frac{\partial}{\partial x'} \\ \frac{\partial^2}{\partial y^2} &= \frac{1}{\left(l'\right)^2}\frac{\partial^2}{\partial x^2} \end{aligned}\right\} \tag{A9}$$

For the insulation layer

$$\left.\begin{aligned} \frac{\partial}{\partial y} &= \frac{1}{l''}\frac{\partial}{\partial x''} \\ \frac{\partial^2}{\partial y^2} &= \frac{1}{(l'')^2}\frac{\partial^2}{(\partial x'')^2} \end{aligned}\right\} \tag{A10}$$

The time derivative in the char-layer equations is transformed as follows

$$\left(\frac{\partial}{\partial t}\right)_{\text{fixed}} = \left(\frac{\partial}{\partial t}\right)_{\text{moving}} + \left(\frac{\partial x}{\partial l}\frac{\partial l}{\partial t} + \frac{\partial x}{\partial t}\right)\frac{\partial}{\partial x} \tag{A11}$$

where

$$\left.\begin{aligned} \frac{\partial x}{\partial l} &= -\frac{x}{l} \\ \frac{\partial x}{\partial t} &= -\frac{1}{l}\frac{\dot{m}_s}{\rho_{s,0}} \\ l &= l_o + \int_0^t \left(\frac{\dot{m}_g}{\Delta\rho} - \frac{\dot{m}_s}{\rho_{s,0}}\right)dt \\ \frac{\partial l}{\partial t} &= \frac{\dot{m}_g}{\Delta\rho} - \frac{\dot{m}_s}{\rho_{s,0}} \end{aligned}\right\} \tag{A12}$$

Therefore

$$\left(\frac{\partial}{\partial t}\right)_{\text{fixed}} = \left(\frac{\partial}{\partial t}\right)_{\text{moving}} - V_c\frac{\partial}{\partial x} \tag{A13}$$

where

$$V_c = \frac{1}{l}\left[\frac{\dot{m}_s}{\rho_{s,0}} + x\left(\frac{\dot{m}_g}{\Delta\rho} - \frac{\dot{m}_s}{\rho_{s,0}}\right)\right] \tag{A14}$$

For the uncharred layer the time derivative is transformed as follows

$$\left(\frac{\partial}{\partial t}\right)_{\text{fixed}} = \left(\frac{\partial}{\partial t}\right)_{\text{moving}} + \left(\frac{\partial x'}{\partial l'}\frac{\partial l'}{\partial t} + \frac{\partial x'}{\partial t}\right)\frac{\partial}{\partial x'} \tag{A15}$$

where

$$\left.\begin{aligned} \frac{\partial x'}{\partial l'} &= -\frac{x'}{l'} \\ \frac{\partial x'}{\partial t} &= -\frac{1}{l'}\frac{\dot{m}_g}{\Delta\rho} \\ l' &= l'_o - \int_0^t \frac{\dot{m}_g}{\Delta\rho}\,dt \\ \frac{\partial l'}{\partial t} &= -\frac{\dot{m}_g}{\Delta\rho} \end{aligned}\right\} \tag{A16}$$

Therefore

$$\left(\frac{\partial}{\partial t}\right)_{\text{fixed}} = \left(\frac{\partial}{\partial t}\right)_{\text{moving}} - \frac{\dot{m}_g}{\Delta\rho}\left(\frac{1 - x'}{l'}\right)\frac{\partial}{\partial x'} \tag{A17}$$

Transformed Differential Equations and Boundary Conditions

The differential equations and boundary conditions in the transformed coordinate system are given in a convenient standardized form in the following sections.

Solid temperature equations and boundary conditions.- The transformed char temperature equation is

$$\frac{\partial^2 T_s}{\partial x^2} + \alpha_1\frac{\partial T_s}{\partial x} + \alpha_2 T_s + \alpha_3 + \alpha_4\frac{\partial T_s}{\partial t} = 0 \tag{A18}$$

where

$$\alpha_1 = \frac{1}{k_s}\left[\frac{\partial k_s}{\partial x} + \rho_s l^2(1 - \eta)C_{p,s}V_c\right] \tag{A19a}$$

$$\alpha_2 = -H_A \frac{l^2}{k_s} \tag{A19b}$$

$$\alpha_3 = \frac{l^2}{k_s}\left\{H_A T + \eta R_s \left[\overline{H(T)}\right]_s + \eta R_{h,s} H_s - \eta \sum_r r_h^{(r)} \Delta H^{(r)} + (1 - \eta)(A - E) + (1 - \eta) q_s''' + \frac{\rho_s H_s}{M_s}\left(\frac{\partial \eta}{\partial t} - l V_c \frac{\partial \eta}{\partial x}\right)\right\} \tag{A19c}$$

$$\alpha_4 = -(1 - \eta) l^2 \frac{\rho_s C_{p,s}}{M_s k_s} \tag{A19d}$$

The transformed temperature equation for the uncharred layer is

$$\frac{\partial^2 T_s'}{(\partial x')^2} + \alpha_1' \frac{\partial T_s'}{\partial x'} + \alpha_2' T_s' + \alpha_3' + \alpha_4' \frac{\partial T_s'}{\partial t} = 0 \tag{A20}$$

where

$$\alpha_1' = \frac{1}{k_s'}\left[\frac{\partial k_s'}{\partial x'} + l' \hat{C}_{p,s}' \rho_s' \frac{\dot{m}_g}{\Delta \rho}(1 - x')\right] \tag{A21a}$$

$$\alpha_2' = 0 \tag{A21b}$$

$$\alpha_3' = 0 \tag{A21c}$$

$$\alpha_4' = -\rho_s' \frac{\hat{C}_{p,s}' (l')^2}{k_s'} \tag{A21d}$$

The transformed temperature equation for the insulation layer is

$$\frac{\partial^2 T_s''}{(\partial x'')^2} + \alpha_1'' \frac{\partial T_s''}{\partial x''} + \alpha_2'' T_s'' + \alpha_3'' + \alpha_4'' \frac{\partial T_s''}{\partial t} = 0 \tag{A22}$$

where

$$\alpha_1'' = \frac{1}{k_s''} \frac{\partial k_s''}{\partial x''} \tag{A23a}$$

$$\alpha_2'' = 0 \tag{A23b}$$

$$\alpha_3'' = 0 \tag{A23c}$$

$$\alpha_4'' = -\rho_s'' \hat{C}_{p,s}'' \frac{(l'')^2}{k_s''} \tag{A23d}$$

The boundary conditions for the solid temperature equations are as follows:

At $x = 0$

$$q_C\left(1 - \frac{H_w}{H_e}\right)\left\{1 - (1 - \beta)\left[0.724 \frac{H_e \dot{m}_T}{q_C \bar{M}_w} - 0.13\left(\frac{H_e \dot{m}_T}{q_C \bar{M}_w}\right)^2\right] - \beta\bar{\eta} \frac{H_e \dot{m}_T}{q_C \bar{M}_w}\right\} + \alpha q_R + \dot{m}_c \Delta H_c$$

$$= \sigma \epsilon_s T_{s,1}^4 - \frac{k_s}{l} \frac{\partial T_s}{\partial x} + S\left(T_{s,1} - \bar{T}_1\right)\dot{m}_{sb} H_c \tag{A24}$$

At $x = 1, \quad x' = 0$

$$T_s = T_s' \tag{A25a}$$

and

$$-\frac{k_s}{l} \frac{\partial T_s}{\partial x} = \dot{m}_g \Delta H_p - \frac{k_s'}{l'} \frac{\partial T_s'}{\partial x'} \tag{A25b}$$

At $x' = 1, \quad x'' = 0$

$$T_s' = T_s'' \tag{A26a}$$

and

$$-\frac{k_s'}{l'} \frac{\partial T_s'}{\partial x'} = -\frac{k_s''}{l''} \frac{\partial T_s''}{\partial x''} + \rho_{HS} \hat{C}_{p,HS} l_{HS} \frac{\partial T_s''}{\partial t} \tag{A26b}$$

At $x'' = 1$

$$-\frac{k_s''}{\ell''}\frac{\partial T_s''}{\partial x''} + q_B = \sigma\epsilon_s''\left(T_s''\right)^4 + \rho_{HSP}\hat{C}_{p,HSP}\ell_{HSP}\frac{\partial T_s''}{\partial t} \tag{A27}$$

Pyrolysis-gas pressure equation and boundary conditions.- The transformed pyrolysis-gas pressure equation is

$$\frac{\partial^2 P^2}{\partial x^2} + \gamma_1\frac{\partial P^2}{\partial x} + \gamma_2 P^2 + \gamma_3 + \gamma_4\frac{\partial P^2}{\partial t} = 0 \tag{A28}$$

where

$$\gamma_1 = \frac{\mu}{K}\left[\frac{T}{\bar{M}}\frac{\partial}{\partial x}\left(\frac{K\bar{M}}{\mu T}\right) + \frac{\eta V_c}{P}\right] \tag{A29a}$$

$$\gamma_2 = -\frac{2\mu}{\bar{M}KP}\left[\eta\left(\frac{\partial\bar{M}}{\partial t} - V_c\frac{\partial\bar{M}}{\partial x}\right) - \eta\frac{\bar{M}}{T}\left(\frac{\partial T}{\partial t} - \frac{\partial T}{\partial x}\right) + \bar{M}\left(\frac{\partial\eta}{\partial t} - V_c\frac{\partial\eta}{\partial x}\right)\right] \tag{A29b}$$

$$\gamma_3 = \frac{2\mu\eta}{K\rho}\sum_i R_{T,i}M_i \tag{A29c}$$

$$\gamma_4 = -\frac{\mu\eta}{KP} \tag{A29d}$$

The boundary conditions for the pyrolysis-gas pressure equation are:

At $x = 0$

$$P = P_w \tag{A30}$$

At $x = 1$

$$\frac{\partial}{\partial x}(P^2) = 2\ell R_u\frac{\mu T}{K\bar{M}}\dot{m}_g \tag{A31}$$

Char porosity equation and boundary condition.- The transformed char porosity equation is

$$\frac{\partial\eta}{\partial x} + E_1\eta + E_2 + E_3\frac{\partial\eta}{\partial t} = 0 \tag{A32}$$

where

$$E_1 = \frac{-M_s\left(R_{h,s} + R_s\right)}{\rho_s V_c} \tag{A33a}$$

$$E_2 = 0 \tag{A33b}$$

$$E_3 = -\frac{1}{lV_c} \tag{A33c}$$

The boundary condition for the char porosity equation is unchanged by the coordinate transformation.

Pyrolysis-gas temperature equation and boundary condition.- The transformed pyrolysis-gas temperature equation is

$$\frac{\partial T}{\partial x} + \beta_1 T + \beta_2 + \beta_3 \frac{\partial T}{\partial t} = 0 \tag{A34}$$

where

$$\beta_1 = \frac{H_A - \eta R_u \left[\frac{\rho}{\eta \overline{M}}\left(\frac{\partial \eta}{\partial t} - V_c \frac{\partial \eta}{\partial x}\right) + \frac{\partial}{\partial t}\left(\sum_i \frac{\rho_i}{M_i}\right) + \left(\frac{v}{l} - V_c\right)\frac{\partial}{\partial x}\left(\sum_i \frac{\rho_i}{M_i}\right)\right]}{\eta\left(\frac{v}{l} - V_c\right)\left(\sum_i \frac{\rho_i C_{p,i}}{M_i} - R_u \sum_i \frac{\rho_i}{M_i}\right)} \tag{A35a}$$

$$\beta_2 = \frac{\eta\left\{\sum_i R_{T,i} H_i - \frac{v^2}{2}\sum_i R_{T,i} M_i + R_s\left[H(T)\right]_s + R_{h,s} H_s - \sum_r r_h^{(r)} \Delta H^{(r)}\right\} - H_A T_s}{\eta\left(\frac{v}{l} - V_c\right)\left(\sum_i \frac{\rho_i C_{p,i}}{M_i} - R_u \sum_i \frac{\rho_i}{M_i}\right)} \tag{A35b}$$

$$\beta_3 = \frac{l}{v - lV_c} \tag{A35c}$$

The boundary condition for the pyrolysis-gas temperature equation is unchanged by the coordinate transformation.

Chemical-species continuity equation and boundary condition.- The transformed chemical-species continuity equation is

$$\frac{\partial}{\partial x}\dot{m}_i + \Delta_{1,i}\dot{m}_i + \Delta_{2,i} + \Delta_{3,i}\frac{\partial}{\partial t}\dot{m}_i = 0 \tag{A36}$$

where

$$\Delta_{1,i} = \frac{\frac{1}{\eta}\frac{\partial \eta}{\partial x} + \left(l\frac{R_{T,i}M_i}{\rho_i} - \frac{l}{\eta}\frac{\partial \eta}{\partial t} - vlV_c\frac{\partial v}{\partial x}\right)}{lV_c - v} \tag{A37a}$$

$$\Delta_{2,i} = \frac{vl\frac{\partial \rho_i}{\partial t}}{lV_c - v} \tag{A37b}$$

$$\Delta_{3,i} = 0 \tag{A37c}$$

The boundary condition for the chemical-species continuity equation is unchanged by the coordinate transformation.

Total-mass conservation equation and boundary condition.- The transformed total-mass conservation equation is

$$\frac{\partial}{\partial x}\dot{m} = l\left[\frac{\partial}{\partial t}(\eta\rho) - \eta\sum_i R_{T,i}M_i - V_c\frac{\partial}{\partial x}(\eta\rho)\right] \tag{A38}$$

It is convenient to integrate this equation numerically rather than use finite-difference methods; hence, it is not expressed in the linear form. The solution to this equation is used with the total density obtained from the equation of state to determine the mass average velocity of the pyrolysis gases. The boundary condition for the total-mass conservation equation is unchanged by the coordinate transformation.

APPENDIX B

FINITE-DIFFERENCE EQUATIONS

The procedure used to solve all equations except the total-mass conservation equation involves converting the governing differential equations to finite-difference form and solving the resulting sets of algebraic equations by iteration. The total-mass conservation equation is solved by numerical integration.

The distances between stations in the char layer, the uncharred layer, and the insulation layer are

$$\left.\begin{aligned} \Delta x &= \frac{1}{I - 1} \\ \Delta x' &= \frac{1}{J} \\ \Delta x'' &= \frac{1}{K} \end{aligned}\right\} \tag{B1}$$

where I, J, and K are the number of stations in the respective layers. The station coordinates are: For the char layer

$$x = (N - 1)\Delta x \tag{B2}$$

For the uncharred layer

$$x' = (N - I)\Delta x' \tag{B3}$$

For the insulation layer

$$x'' = (N - I - J)\Delta x'' \tag{B4}$$

Solid-Phase Temperature Equations

The differential equation for the char temperature is

$$\frac{\partial^2 T_s}{\partial x^2} + \alpha_1 \frac{\partial T_s}{\partial x} + \alpha_2 T_s + \alpha_3 + \alpha_4 \frac{\partial T_s}{\partial t} = 0 \tag{B5}$$

Interior stations of char layer.- At interior stations the partial derivatives are replaced by central-difference approximations. The central-difference approximations of the partial derivative are obtained from Taylor series expansions at the station N evaluated at $N + 1$ and $N - 1$. Thus

$$\left(\frac{\partial T_s}{\partial x}\right)_N = \frac{T_s(N + 1) - T_s(N - 1)}{2\Delta x} \tag{B6}$$

which is accurate to terms of the order of Δx^2 and

$$\left(\frac{\partial^2 T_s}{\partial x^2}\right)_N = \frac{T_s(N - 1) - 2T_s(N) + T_s(N + 1)}{\Delta x^2} \tag{B7}$$

which is accurate to terms of the order Δx^2.

Equations (B6) and (B7) are used in equation (B5) to obtain

$$\frac{1}{\Delta x^2}\left[T_s(N - 1) - 2T_s(N) + T_s(N + 1)\right] + \frac{\alpha_1(N)}{2\Delta x}\left[T_s(N + 1) - T_s(N - 1)\right]$$

$$+ \alpha_2(N)\, T_s(N) + \alpha_3(N) + \alpha_4(N)\left(\frac{\partial T_s}{\partial t}\right)_N = 0 \tag{B8}$$

The finite-difference approximation of the time derivative in equation (B8) is obtained from Taylor series expansions at time $P + (\Delta t/2)$ evaluated at time P and $P + \Delta t$. Thus

$$\left(\alpha_4 \frac{\partial T_s}{\partial t}\right)^{P+(\Delta t/2)} = \frac{1}{2}\left[\alpha_4^P\left(\frac{\partial T_s}{\partial t}\right)^P + \alpha_4^{P+\Delta t}\left(\frac{\partial T_s}{\partial t}\right)^{P+\Delta t}\right] \tag{B9}$$

which is accurate to terms of the order Δt^2. Now

$$\left(\alpha_4 \frac{\partial T_s}{\partial t}\right)^{P+(\Delta t/2)} = \alpha_4^{P+(\Delta t/2)}\left(\frac{\partial T_s}{\partial t}\right)^{P+(\Delta t/2)} \tag{B10}$$

where

$$\alpha_4^{P+(\Delta t/2)} = \frac{1}{2}\left(\alpha_4^{P} + \alpha_4^{P+\Delta t}\right) \tag{B11}$$

and

$$\left(\frac{\partial T_s}{\partial t}\right)^{P+(\Delta t/2)} = \frac{T_s^{P+\Delta t} - T_s^{P}}{\Delta t} \tag{B12}$$

Combining equations (B8) to (B12) gives

$$A_s(N)\, T_s(N-1)^{P+\Delta t} + B_s(N)\, T_s(N)^{P+\Delta t} + C_s(N)\, T_s(N+1)^{P+\Delta t} = D_s(N) \tag{B13}$$

where

$$A_s(N) = \frac{1}{2}\left[\frac{1}{\Delta x^2} - \frac{\alpha_1(N)^{P+\Delta t}}{2\Delta x}\right] \tag{B14a}$$

$$B_s(N) = \frac{1}{2}\left\{\alpha_2(N)^{P+\Delta t} - \frac{2}{\Delta x^2} + \frac{1}{\Delta t}\left[\alpha_4(N)^{P} + \alpha_4(N)^{P+\Delta t}\right]\right\} \tag{B14b}$$

$$C_s(N) = \frac{1}{2\Delta x^2} + \frac{\alpha_1(N)^{P+\Delta t}}{4\Delta x} \tag{B14c}$$

$$\begin{aligned} D_s(N) = {} & -\frac{1}{2}\left[\alpha_3(N)^{P} + \alpha_3(N)^{P+\Delta t}\right] - \frac{1}{2}\left[\frac{1}{\Delta x^2} - \frac{\alpha_1(N)^{P}}{2\Delta x}\right] T_s(N-1)^{P} \\ & - \frac{1}{2}\left\{\alpha_2(N)^{P} - \frac{2}{\Delta x^2} - \frac{1}{\Delta t}\left[\alpha_4(N)^{P} + \alpha_4(N)^{P+\Delta t}\right]\right\} T_s(N)^{P} \\ & - \frac{1}{2}\left[\frac{1}{\Delta x^2} + \frac{\alpha_1(N)^{P}}{2\Delta x}\right] T_s(N+1)^{P} \end{aligned} \tag{B14d}$$

Interior stations of uncharred layer.- The modified implicit finite-difference equation at interior stations of the uncharred layer is obtained in a similar way. The resulting equation is

$$A'_s(N)\, T_s(N-1)^{P+\Delta t} + B'_s(N)\, T_s(N)^{P+\Delta t} + C'_s(N)\, T_s(N+1)^{P+\Delta t} = D'_s(N) \tag{B15}$$

where

$$A'_s(N) = \frac{1}{2}\left[\frac{1}{(\Delta x')^2} - \frac{\alpha_1(N)^{P+\Delta t}}{2\Delta x'}\right] \tag{B16a}$$

$$B'_s(N) = \frac{1}{2}\left\{\alpha'_2(N)^{P+\Delta t} - \frac{2}{(\Delta x')^2} + \frac{1}{\Delta t}\left[\alpha'_4(N)^{P} + \alpha'_4(N)^{P+\Delta t}\right]\right\} \tag{B16b}$$

$$C'_s(N) = \frac{1}{2}\left[\frac{1}{(\Delta x')^2} + \frac{\alpha_1(N)^{P+\Delta t}}{2\Delta x'}\right] \tag{B16c}$$

$$\begin{aligned} D'_s(N) = {} & -\frac{1}{2}\left[\alpha'_3(N)^{P} + \alpha'_3(N)^{P+\Delta t}\right] - \frac{1}{2}\left[\frac{1}{(\Delta x')^2} - \frac{\alpha'_1(N)^{P}}{2\Delta x'}\right] T_s(N-1)^{P} \\ & - \frac{1}{2}\left\{\alpha'_2(N)^{P} - \frac{2}{(\Delta x')^2} - \frac{1}{\Delta t}\left[\alpha'_4(N)^{P} + \alpha'_4(N)^{P+\Delta t}\right]\right\} T_s(N)^{P} \\ & - \frac{1}{2}\left[\frac{1}{(\Delta x')^2} + \frac{\alpha'_1(N)^{P}}{2\Delta x'}\right] T_s(N+1)^{P} \end{aligned} \tag{B16d}$$

Interior stations of insulation.- The modified implicit finite-difference equation at interior stations of the insulation layer is similarly obtained as

$$A''_s(N)\, T_s(N-1)^{P+\Delta t} + B''_s(N)\, T_s(N)^{P+\Delta t} + C''_s(N)\, T_s(N+1)^{P+\Delta t} = D''_s(N) \tag{B17}$$

where

$$A_s''(N) = \frac{1}{2}\left[\frac{1}{(\Delta x'')^2} - \frac{\alpha_1''(N)^{P+\Delta t}}{2\Delta x''}\right] \tag{B18a}$$

$$B_s''(N) = \frac{1}{2}\left\{\alpha_2''(N)^{P+\Delta t} - \frac{2}{(\Delta x'')^2} + \frac{1}{\Delta t}\left[\alpha_4''(N)^{P} + \alpha_4''(N)^{P+\Delta t}\right]\right\} \tag{B18b}$$

$$C_s''(N) = \frac{1}{2}\left[\frac{1}{(\Delta x'')^2} + \frac{\alpha_1''(N)^{P+\Delta t}}{2\Delta x''}\right] \tag{B18c}$$

$$\begin{aligned} D_s''(N) = {} & -\frac{1}{2}\left[\alpha_3''(N)^{P} + \alpha_3''(N)^{P+\Delta t}\right] - \frac{1}{2}\left[\frac{1}{(\Delta x'')^2} - \frac{\alpha_1''(N)^{P}}{2\Delta x''}\right] T_s(N-1)^P \\ & - \frac{1}{2}\left\{\alpha_2''(N)^{P} - \frac{2}{(\Delta x'')^2} - \frac{1}{\Delta t}\left[\alpha_4''(N)^{P} + \alpha_4''(N)^{P+\Delta t}\right]\right\} T_s(N)^P \\ & - \frac{1}{2}\left[\frac{1}{(\Delta x'')^2} + \frac{\alpha_1''(N)^{P}}{2\Delta x''}\right] T_s(N+1)^P \end{aligned} \tag{B18d}$$

Boundary stations.- Each boundary-condition equation and the corresponding governing differential equation are combined to obtain a differential equation which is valid only at the boundary. The solution of this equation satisfies both the boundary condition and the governing differential equation.

At front surface (N = 1).- The front-surface boundary condition is

$$-\frac{1}{l}\left(k_s \frac{\partial T_s}{\partial x}\right)_{N=1} = q_{AERO} + \dot{m}_c \Delta H_c - S\left(T_{s,1} - \bar{T}_1\right)\dot{m}_{sb} H_c - \sigma \epsilon_s T_{s,1}^4 \tag{B19a}$$

where

$$q_{AERO} = q_{C,net} + \alpha q_R \tag{B19b}$$

The usual procedure at this point would be to combine the boundary condition with the differential equation for the char layer (eq. (A18))

$$\frac{\partial^2 T_s}{\partial x^2} + \alpha_1 \frac{\partial T_s}{\partial x} + \alpha_2 T_s + \alpha_3 + \alpha_4 \frac{\partial T_s}{\partial t} = 0 \tag{B20}$$

by inserting the boundary condition in place of the first derivative. However since the coefficient α_1 is quite small for most ablator systems, this method does not give good results. This problem is overcome by including the boundary condition in the second-derivative term $\frac{\partial^2 T_s}{\partial x^2}$.

The second-order term in equation (B20) is written as

$$\frac{\partial^2 T_s}{\partial x^2} = \frac{\partial}{\partial x}\left(\frac{\partial T_s}{\partial x}\right) \tag{B21}$$

The derivative of the temperature gradient is obtained from Taylor series expansions at the station $N = 1$ evaluated at $N = 2$, $N = 3$, and $N = 4$. Thus

$$\left[\frac{\partial}{\partial x}\left(\frac{\partial T_s}{\partial x}\right)\right]_{N=1} = \frac{1}{6\Delta x}\left[-11\left(\frac{\partial T_s}{\partial x}\right)_{N=1} + 18\left(\frac{\partial T_s}{\partial x}\right)_{N=2} - 9\left(\frac{\partial T_s}{\partial x}\right)_{N=3} + 2\left(\frac{\partial T_s}{\partial x}\right)_{N=4}\right] \tag{B22}$$

Equations (B19) to (B22) are combined to obtain the finite-difference equation at the surface

$$\left\{\left[\alpha_1(1) - \frac{11}{6\Delta x}\right]\frac{l}{k_s(1)}\sigma\epsilon_s T_s(1)^3 - \frac{3}{2\Delta x^2} + \alpha_1(1)\right\} T_s(1) + \frac{3}{4\Delta x^2} T_s(2)$$

$$+ \frac{4}{3\Delta x^2} T_s(3) - \frac{3}{4\Delta x^2} T_s(4) + \frac{1}{6\Delta x^2} T_s(5) + \alpha_3(1) - \frac{q_{c,net}\, l}{k_s(1)}\left[\alpha_1(1)\right.$$

$$\left. - \frac{11}{6\Delta x}\right] + \alpha_4(1)\left(\frac{\partial T_s}{\partial t}\right)_{N=1} = 0 \tag{B23}$$

Following the procedure used to obtain the modified implicit finite-difference equation for interior stations, the analogous equation for the station at the front surface is

$$B1_s T_s(1)^{P+\Delta t} + C1_s T_s(2)^{P+\Delta t} + G1_s T_s(3)^{P+\Delta t} + H1_s T_s(4)^{P+\Delta t} + I1_s T_s(5)^{P+\Delta t} = D1_s \tag{B24}$$

where

$$B1_s = \left[\alpha_1(1)^{P+\Delta t} - \frac{11}{6\Delta x}\right]\frac{l^{P+\Delta t}\sigma\epsilon_s}{k_s(1)^{P+\Delta t}}\left[T_s(1)^{P+\Delta t}\right]^3 - \frac{3}{2\Delta x^2} + \alpha_2(1)^{P+\Delta t}$$

$$+ \frac{1}{\Delta t}\left[\alpha_4(1)^P + \alpha_4(1)^{P+\Delta t}\right] \tag{B25a}$$

$$C1_s = \frac{3}{8\Delta x^2} \tag{B25b}$$

$$G1_s = \frac{2}{3\Delta x^2} \tag{B25c}$$

$$H1_s = -\frac{3}{8\Delta x^2} \tag{B25d}$$

$$I1_s = \frac{1}{12\Delta x^2} \tag{B25e}$$

$$D1_s = -\alpha_3(1)^P - \alpha_3(1)^{P+\Delta t} + \left[\alpha_1(1)^{P+\Delta t} - \frac{11}{6\Delta x}\right]q_{C,net}^{P+\Delta t}\frac{l^{P+\Delta t}}{k_s(1)^{P+\Delta t}} + \left[\alpha_1(1)^P\right.$$

$$\left. - \frac{11}{6\Delta x}\right]q_{C,net}^{P}\frac{l^P}{k_s(1)^P} - \left\{\left[\alpha_1(1)^P - \frac{11}{6\Delta x}\right]\frac{l^P\sigma\epsilon_s}{k_s(1)^P}\left[T_s(1)^P\right]^3 - \frac{3}{2\Delta x^2} + \alpha_2(1)^P\right.$$

$$\left. - \frac{1}{\Delta t}\left[\alpha_4(1)^P + \alpha_4(1)^{P+\Delta t}\right]\right\}T_s(1)^P - \frac{3}{4\Delta x^2}T_s(2)^P - \frac{4}{3\Delta x^2}T_s(3)^P$$

$$+ \frac{3}{4\Delta x^2}T_s(4)^P - \frac{1}{6\Delta x^2}T_s(5)^P \tag{B25f}$$

At pyrolysis zone (N = I).- The boundary condition at the pyrolysis zone is

$$-\frac{1}{l}\left(k_s \frac{\partial T_s}{\partial x}\right)_{N=I} = \dot{m}_g \Delta H_p - \frac{1}{l'}\left(k'_s \frac{\partial T_s}{\partial x'}\right)_{N=I} \tag{B26}$$

Equation (B26) is combined with the differential equations for conservation of the char layer and the uncharred layer in the same manner as the surface boundary condition was combined with the char-layer equation to obtain the following modified implicit finite-difference equation

$$ZI_s T_s(I-4)^{P+\Delta t} + YI_s T_s(I-3)^{P+\Delta t} + XI_s T_s(I-2)^{P+\Delta t} + AI_s T_s(I-1)^{P+\Delta t}$$
$$+ BI_s T_s(I)^{P+\Delta t} + CI_s T_s(I+1)^{P+\Delta t} + EI_s T_s(I+2)^{P+\Delta t} + FI_s T_s(I+3)^{P+\Delta t}$$
$$+ GI_s T_s(I+4)^{P+\Delta t} = DI_s \tag{B27}$$

where

$$ZI_s = \frac{-k_s(I)^{P+\Delta t} \Big/ \left(12\Delta x l^{P+\Delta t}\right)}{\dfrac{k_s(I)^{P+\Delta t}\alpha_4(I)^{P+\Delta t}\Delta x}{l^{P+\Delta t}} + \dfrac{k'_s(I)^{P+\Delta t}\alpha'_4(I)^{P+\Delta t}\Delta x'}{(l')^{P+\Delta t}}} \tag{B28a}$$

$$YI_s = \frac{k_s(I)^{P+\Delta t}\left[\dfrac{3}{4\Delta x} + \dfrac{\alpha_1(I)^{P+\Delta t}}{3}\right] \Big/ l^{P+\Delta t}}{2\left[\dfrac{k_s(I)^{P+\Delta t}\alpha_4(I)^{P+\Delta t}\Delta x}{l^{P+\Delta t}} + \dfrac{k'_s(I)^{P+\Delta t}\alpha'_4(I)^{P+\Delta t}\Delta x'}{(l')^{P+\Delta t}}\right]} \tag{B28b}$$

$$XI_s = \frac{-k_s(I)^{P+\Delta t}\left[\dfrac{4}{3\Delta x} + \dfrac{3\alpha_1(x)^{P+\Delta t}}{2}\right] \Big/ l^{P+\Delta t}}{2\left[\dfrac{k_s(I)^{P+\Delta t}\alpha_4(I)^{P+\Delta t}\Delta x}{l^{P+\Delta t}} + \dfrac{k'_s(I)^{P+\Delta t}\alpha'_4(I)^{P+\Delta t}\Delta x'}{(l')^{P+\Delta t}}\right]} \tag{B28c}$$

$$AI_S = \frac{-k_s(I)^{P+\Delta t}\left[\frac{3}{4\Delta x} - 3\alpha_1(I)^{P+\Delta t}\right] \Big/ l^{P+\Delta t}}{2\left[\frac{k_s(I)^{P+\Delta t}\alpha_4(I)^{P+\Delta t}\Delta x}{l^{P+\Delta t}} + \frac{k'_s(I)^{P+\Delta t}\alpha'_4(I)^{P+\Delta t}\Delta x'}{(l')^{P+\Delta t}}\right]} \tag{B28d}$$

$$BI_S = -\frac{1}{\Delta t} + \frac{1}{2\left[\frac{k_s(I)^{P+\Delta t}\alpha_4(I)^{P+\Delta t}\Delta x}{l^{P+\Delta t}} + \frac{k'_s(I)^{P+\Delta t}\alpha'_4(I)^{P+\Delta t}\Delta x'}{(l')^{P+\Delta t}}\right]} \left\{ \frac{k_s(I)^{P+\Delta t}}{l^{P+\Delta t}} \left[\frac{3}{2\Delta x} - \frac{11}{6}\alpha_1(I)^{P+\Delta t} - \alpha_2(I)^{P+\Delta t}\Delta x \right] + \frac{k'_s(I)^{P+\Delta t}}{(l')^{P+\Delta t}} \left[\frac{3}{2\Delta x'} + \frac{11}{6}\alpha'_1(I)^{P+\Delta t} - \alpha'_2(I)^{P+\Delta t} \right] \right\} \tag{B28e}$$

$$CI_S = \frac{-k'_s(I)^{P+\Delta t}\left[\frac{3}{4\Delta x'} + 3\alpha'_1(I)^{P+\Delta t}\right] \Big/ (l')^{P+\Delta t}}{2\left[\frac{k_s(I)^{P+\Delta t}\alpha_4(I)^{P+\Delta t}\Delta x}{l^{P+\Delta t}} + \frac{k'_s(I)^{P+\Delta t}\alpha'_4(I)^{P+\Delta t}\Delta x'}{(l')^{P+\Delta t}}\right]} \tag{B28f}$$

$$EI_S = \frac{-k'_s(I)^{P+\Delta t}\left[\frac{4}{3\Delta x'} + 3\alpha'_1(I)^{P+\Delta t}\right] \Big/ (l')^{P+\Delta t}}{2\left[\frac{k_s(I)^{P+\Delta t}\alpha_4(I)^{P+\Delta t}\Delta x}{l^{P+\Delta t}} + \frac{k'_s(I)^{P+\Delta t}\alpha'_4(I)^{P+\Delta t}\Delta x'}{(l')^{P+\Delta t}}\right]} \tag{B28g}$$

$$FI_S = \frac{-k'_s(I)^{P+\Delta t}\left[\frac{3}{4\Delta x'} - \frac{1}{3}\alpha'_1(I)^{P+\Delta t}\right] \Big/ (l')^{P+\Delta t}}{2\left[\frac{k_s(I)^{P+\Delta t}\alpha_4(I)^{P+\Delta t}\Delta x}{l^{P+\Delta t}} + \frac{k'_s(I)^{P+\Delta t}\alpha'_4(I)^{P+\Delta t}\Delta x'}{(l')^{P+\Delta t}}\right]} \tag{B28h}$$

$$GI_S = \frac{-k'_s(I)^{P+\Delta t} \Big/ \left[12\Delta x'(l')^{P+\Delta t}\right]}{\dfrac{k_s(I)^{P+\Delta t}\alpha_4(I)^{P+\Delta t}\Delta x}{l^{P+\Delta t}} + \dfrac{k'_s(I)^{P+\Delta t}\alpha'_4(I)^{P+\Delta t}\Delta x'}{(l')^{P+\Delta t}}} \tag{B28i}$$

$$DI_S = \frac{1}{2\left[\dfrac{k_s(I)^{P+\Delta t}\alpha_4(I)^{P+\Delta t}\Delta x}{l^{P+\Delta t}} + \dfrac{k'_s(I)^{P+\Delta t}\alpha'_4(I)^{P+\Delta t}\Delta x'}{(l')^{P+\Delta t}}\right]}\left[\frac{k_s(I)^{P+\Delta t}\alpha_3(I)^{P+\Delta t}\Delta x}{l^{P+\Delta t}} + \frac{k'_s(I)^{P+\Delta t}\alpha'_3(I)^{P+\Delta t}\Delta x'}{(l')^{P+\Delta t}} - \frac{11}{6}\dot{m}_g^{P+\Delta t}\Delta H_p\right] + \frac{1}{2\left[\dfrac{k_s(I)^P\alpha_4(I)^P\Delta x}{l^P} + \dfrac{k'_s(I)^P\alpha'_4(I)^P\Delta x'}{(l')^P}\right]}$$

$$\times\left[\frac{k_s(I)^P\alpha_3(I)^P\Delta x}{l^P} + \frac{k'_s(I)^P\alpha'_3(I)^P\Delta x'}{(l')^P} - \frac{11}{6}\dot{m}_g^P\Delta H_p\right]$$

$$- \frac{k_s(I)^P \Big/ l^P}{2\left[\dfrac{k_s(I)^P\alpha_4(I)^P\Delta x}{l^P} + \dfrac{k'_s(I)^P\alpha'_4(I)^P\Delta x'}{(l')^P}\right]}\left\{-\frac{1}{6\Delta x}T_s(I-4)^P + \left[\frac{3}{4\Delta x} + \frac{\alpha_1(I)^P}{3}\right]T_s(I-3)^P\right.$$

$$\left. - \left[\frac{4}{3\Delta x} + \frac{3}{2}\alpha_1(I)^P\right]T_s(I-2)^P - \left[\frac{3}{4\Delta x} - 3\alpha_1(I)^P\right]T_s(I-1)^P\right\}$$

$$- \left(\frac{1}{2\left[\dfrac{k_s(I)^P\alpha_4(I)^P\Delta x}{l^P} + \dfrac{k'_s(I)^P\alpha'_4(I)^P\Delta x'}{(l')^P}\right]}\left\{\frac{k_s(I)^P}{l^P}\left[\frac{3}{2\Delta x} - \frac{11}{6}\alpha_1(I)^P - \alpha_2(I)^P\Delta x\right]\right.\right.$$

(Equation continued on next page)

$$+\frac{k'_s(I)^P}{(l')^P}\left[\frac{3}{2\Delta x'}+\frac{11}{6}\alpha'_1(I)^P-\alpha'_2(I)^P\Delta x'\right]\Bigg\}+\frac{1}{\Delta t}\Bigg)T_s(I)^P$$

$$+\frac{k'_s(I)^P/(l')^P}{2\left[\dfrac{k_s(I)^P\alpha_4(I)^P\Delta x}{l^P}+\dfrac{k'_s(I)^P\alpha'_4(I)^P\Delta x'}{(l')^P}\right]}\Bigg\{\left[\frac{3}{4\Delta x'}+3\alpha'_1(I)^P\right]T_s(I+1)^P+\left[\frac{4}{3\Delta x'}\right.$$

$$\left.-\frac{3}{2}\alpha'_1(I)^P\right]T_s(I+2)^P-\left[\frac{3}{4\Delta x'}-\frac{1}{3}\alpha'_1(I)^P\right]T_s(I+3)^P+\frac{1}{6\Delta x'}T_s(I+4)^P\Bigg\} \qquad \text{(B28j)}$$

At uncharred-material—insulation interface (N = I + J).- The boundary condition at the interface of the uncharred material and the insulation is

$$-\frac{1}{l'}\left(k'_s\frac{\partial T_s}{\partial x'}\right)_{N=I+J}=-\frac{1}{l''}\left(k''_s\frac{\partial T_s}{\partial x''}\right)_{N=I+J}+\rho_{HS}\hat{C}_{p,HS}l_{HS}\left(\frac{\partial T_s}{\partial t}\right)_{N=I+J} \qquad \text{(B29)}$$

Equation (B29) is combined with the uncharred-material temperature equation and the insulation-material equation by following the procedure used for the pyrolysis-zone equations. The resulting modified implicit finite-difference equation is

$$ZP_sT_s(I+J-4)^{P+\Delta t}+YP_sT_s(I+J-3)^{P+\Delta t}+XP_sT_s(I+J-2)^{P+\Delta t}$$

$$+AP_sT_s(I+J-1)^{P+\Delta t}+BP_sT_s(I+J)^{P+\Delta t}+CP_sT_s(I+J+1)^{P+\Delta t}$$

$$+EP_sT_s(I+J+2)^{P+\Delta t}+FP_sT_s(I+J+3)^{P+\Delta t}+GP_sT_s(I+J+4)^{P+\Delta t}=DP_s \qquad \text{(B30)}$$

where

$$ZP_s=\frac{k'_s(I+J)^{P+\Delta t}/\left[12\Delta x'(l')^{P+\Delta t}\right]}{\dfrac{k'_s(I+J)^{P+\Delta t}\alpha'_4(I+J)^{P+\Delta t}\Delta x'}{(l')^{P+\Delta t}}+\dfrac{k''_s(I+J)^{P+\Delta t}\alpha''_4(I+J)^{P+\Delta t}\Delta x''}{(l'')^{P+\Delta t}}-\rho_{HS}\hat{C}_{p,HS}l_{HS}} \qquad \text{(B31a)}$$

$$YP_S = \frac{k'_s(I+J)^{P+\Delta t} \Big/ (l')^{P+\Delta t}\left[\frac{3}{4\Delta x'} + \frac{\alpha'_1(I+J)^{P+\Delta t}}{3}\right]}{2\left[\frac{k'_s(I+J)^{P+\Delta t}\alpha'_4(I+J)^{P+\Delta t}\Delta x'}{(l')^{P+\Delta t}} + \frac{k''_s(I+J)^{P+\Delta t}\alpha''_4(I+J)^{P+\Delta t}\Delta x''}{(l'')^{P+\Delta t}} - \rho_{HS}\hat{C}_{p,HS}l_{HS}\right]} \tag{B31b}$$

$$XP_S = \frac{-k'_s(I+J)^{P+\Delta t} \Big/ (l')^{P+\Delta t}\left[\frac{4}{3\Delta x'} + \frac{3}{2}\alpha'_1(I+J)^{P+\Delta t}\right]}{2\left[\frac{k'_s(I+J)^{P+\Delta t}\alpha'_4(I+J)^{P+\Delta t}\Delta x'}{(l')^{P+\Delta t}} + \frac{k''_s(I+J)^{P+\Delta t}\alpha''_4(I+J)^{P+\Delta t}\Delta x''}{(l'')^{P+\Delta t}} - \rho_{HS}\hat{C}_{p,HS}l_{HS}\right]} \tag{B31c}$$

$$AP_S = \frac{-k'_s(I+J)^{P+\Delta t} \Big/ (l')^{P+\Delta t}\left[\frac{3}{4\Delta x'} - 3\alpha'_1(I+J)^{P+\Delta t}\right]}{2\left[\frac{k'_s(I+J)^{P+\Delta t}\alpha'_4(I+J)^{P+\Delta t}\Delta x'}{(l')^{P+\Delta t}} + \frac{k''_s(I+J)^{P+\Delta t}\alpha''_4(I+J)^{P+\Delta t}\Delta x''}{(l'')^{P+\Delta t}} - \rho_{HS}\hat{C}_{p,HS}l_{HS}\right]} \tag{B31d}$$

$$BP_S = \frac{1}{2\left[\frac{k'_s(I+J)^{P+\Delta t}\alpha'_4(I+J)^{P+\Delta t}\Delta x'}{(l')^{P+\Delta t}} + \frac{k''_s(I+J)^{P+\Delta t}\alpha''_4(I+J)^{P+\Delta t}\Delta x''}{(l'')^{P+\Delta t}} - \rho_{HS}\hat{C}_{p,HS}l_{HS}\right]}$$

$$\times \left\{ \frac{k'_s(I+J)^{P+\Delta t}}{(l')^{P+\Delta t}}\left[\frac{3}{2\Delta x'} - \frac{11}{6}\alpha'_1(I+J)^{P+\Delta t} - \alpha'_2(I+J)^{P+\Delta t}\Delta x'\right] + \frac{k''_s(I+J)^{P+\Delta t}}{(l'')^{P+\Delta t}} \right.$$

$$\left. \times \left[\frac{3}{2\Delta x''} + \frac{11}{6}\alpha''_1(I+J)^{P+\Delta t} - \alpha''_2(I+J)^{P+\Delta t}\Delta x''\right] \right\} - \frac{1}{\Delta t} \tag{B31e}$$

$$CP_S = \frac{-k_s''(I+J)^{P+\Delta t} \Big/ (l'')^{P+\Delta t}\left[\frac{3}{4\Delta x''} + 3\alpha_1''(I+J)^{P+\Delta t}\right]}{2\left[\frac{k_s'(I+J)^{P+\Delta t}\alpha_4'(I+J)^{P+\Delta t}\Delta x'}{(l')^{P+\Delta t}} + \frac{k_s''(I+J)^{P+\Delta t}\alpha_4''(I+J)^{P+\Delta t}\Delta x''}{(l'')^{P+\Delta t}} - \rho_{HS}\hat{C}_{p,HS}{}^{l}{}_{HS}\right]} \quad \text{(B31f)}$$

$$EP_S = \frac{-k_s''(I+J)^{P+\Delta t} \Big/ (l'')^{P+\Delta t}\left[\frac{4}{3\Delta x''} - \frac{3}{2}\alpha_1''(I+J)^{P+\Delta t}\right]}{2\left[\frac{k_s'(I+J)^{P+\Delta t}\alpha_4'(I+J)^{P+\Delta t}\Delta x'}{(l')^{P+\Delta t}} + \frac{k_s''(I+J)^{P+\Delta t}\alpha_4''(I+J)^{P+\Delta t}\Delta x''}{(l'')^{P+\Delta t}} - \rho_{HS}\hat{C}_{p,HS}{}^{l}{}_{HS}\right]} \quad \text{(B31g)}$$

$$FP_S = \frac{-k_s''(I+J)^{P+\Delta t} \Big/ (l'')^{P+\Delta t}\left[\frac{3}{4\Delta x''} - \frac{1}{3}\alpha_1''(I+J)^{P+\Delta t}\right]}{2\left[\frac{k_s'(I+J)^{P+\Delta t}\alpha_4'(I+J)^{P+\Delta t}\Delta x'}{(l')^{P+\Delta t}} + \frac{k_s''(I+J)^{P+\Delta t}\alpha_4''(I+J)^{P+\Delta t}\Delta x''}{(l'')^{P+\Delta t}} - \rho_{HS}\hat{C}_{p,HS}{}^{l}{}_{HS}\right]} \quad \text{(B31h)}$$

$$GP_S = \frac{-k_s''(I+J)^{P+\Delta t} \Big/ \left[12\Delta x''(l'')^{P+\Delta t}\right]}{\frac{k_s'(I+J)^{P+\Delta t}\alpha_4'(I+J)^{P+\Delta t}\Delta x'}{(l')^{P+\Delta t}} + \frac{k_s''(I+J)^{P+\Delta t}\alpha_4''(I+J)^{P+\Delta t}\Delta x''}{(l'')^{P+\Delta t}} - \rho_{HS}\hat{C}_{p,HS}{}^{l}{}_{HS}} \quad \text{(B31i)}$$

$$DP_S = \frac{k_s'(I+J)^{P+\Delta t}\alpha_3'(I+J)^{P+\Delta t}\Delta x' \Big/ (l')^{P+\Delta t} + k_s''(I+J)^{P+\Delta t}\alpha_3''(I+J)^{P+\Delta t}\Delta x'' \Big/ (l'')^{P+\Delta t}}{2\left[\frac{k_s'(I+J)^{P+\Delta t}\alpha_4'(I+J)^{P+\Delta t}\Delta x'}{(l')^{P+\Delta t}} + \frac{k_s''(I+J)^{P+\Delta t}\alpha_4''(I+J)^{P+\Delta t}\Delta x''}{(l'')^{P+\Delta t}} - \rho_{HS}\hat{C}_{p,HS}{}^{l}{}_{HS}\right]}$$

(Equation continued on next page)

$$
- \frac{k_s'(I+J)^P \Big/ (l')^P}{2\left[\dfrac{k_s'(I+J)^{P+\Delta t}\alpha_4'(I+J)^{P+\Delta t}\Delta x'}{(l')^{P+\Delta t}} + \dfrac{k_s''(I+J)^{P+\Delta t}\alpha_4''(I+J)^{P+\Delta t}\Delta x''}{(l'')^{P+\Delta t}} - \rho_{HS}\hat{C}_{p,HS}l_{HS}\right]}
$$

$$
\times \left\{ -\frac{1}{6\Delta x'} T_s(I+J-4)^P + \left[\frac{3}{4\Delta x'} + \frac{1}{3}\alpha_1'(I+J)^P\right] T_s(I+J-3)^P \right.
$$

$$
\left. - \left[\frac{4}{3\Delta x'} + \frac{3}{2}\alpha_1'(I+J)^P\right] T_s(I+J-2)^P - \left[\frac{3}{4\Delta x'} - 3\alpha_1'(I+J)^P\right] T_s(I+J-1)^P \right\}
$$

$$
- \left(\frac{1}{2\left[\dfrac{k_s'(I+J)^P\alpha_4'(I+J)^P\Delta x'}{(l')^P} + \dfrac{k_s''(I+J)^P\alpha_4''(I+J)^P\Delta x''}{(l'')^P} - \rho_{HS}\hat{C}_{p,HS}l_{HS}\right]} \right.
$$

$$
\times \left\{ \frac{k_s'(I+J)^P}{(l')^P}\left[\frac{3}{2\Delta x'} - \frac{11}{6}\alpha_1'(I+J)^P - \alpha_2'(I+J)^P\Delta x'\right] + \frac{k_s''(I+J)^P}{(l'')^P}\left[\frac{3}{2\Delta x''}\right.\right.
$$

$$
\left.\left. + \frac{11}{6}\alpha_1''(I+J)^P - \alpha_2''(I+J)^P\Delta x''\right]\right\} + \left.\frac{1}{\Delta t}\right) T_s(I+J)^P
$$

$$
+ \frac{k_s''(I+J)^P \Big/ (l'')^P}{2\left[\dfrac{k_s'(I+J)^P\alpha_4'(I+J)^P\Delta x'}{(l')^P} + \dfrac{k_s''(I+J)^P\alpha_4''(I+J)^P\Delta x''}{(l'')^P} - \rho_{HS}\hat{C}_{p,HS}l_{HS}\right]}
$$

$$
\times \left\{ \left[\frac{3}{4\Delta x''} + 3\alpha_1''(I+J)^P\right] T_s(I+J+1)^P + \left[\frac{4}{3\Delta x''} - \frac{3}{2}\alpha_1''(I+J)^P\right] T_s(I+J+2)^P \right.
$$

$$
\left. - \left[\frac{3}{4\Delta x''} - \frac{1}{3}\alpha_1''(I+J)\right] T_s(I+J+3)^P + \frac{1}{6\Delta x''} T_s(I+J+4)^P \right\} \qquad \text{(B31j)}
$$

At back surface (N = I + J + K).- The back-surface boundary condition is

$$-\frac{1}{l''}\left(k_s''\frac{\partial T_s}{\partial x''}\right)_{N=I+J+K} = \sigma\epsilon_s''T_s(I+J+K)^4 - q_B + \rho_{HSP}\hat{C}_{p,HSP}l_{HSP}\left(\frac{\partial T_s}{\partial t}\right)_{N=I+J+K} \tag{B32}$$

Equation (B32) is combined with the insulation-material equation. The resulting modified implicit finite-difference equation is

$$ZZ_sT_s(I+J+K-4)^{P+\Delta t} + YZ_sT_s(I+J+K-3)^{P+\Delta t} + XZ_sT_s(I+J+K-2)^{P+\Delta t}$$

$$+ AZ_sT_s(I+J+K-1)^{P+\Delta t} + BZ_sT_s(I+J+K)^{P+\Delta t} = DZ_s \tag{B33}$$

where

$$ZZ_s = \frac{k_s''(I+J+K)^{P+\Delta t}\Big/\left[12(\Delta x'')^2 l''\right]}{\rho_{HSP}\hat{C}_{p,HSP}l_{HSP}\left[\alpha_1''(I+J+K)^{P+\Delta t} + \frac{11}{6\Delta x''}\right] - \frac{\alpha_4''(I+J+K)^{P+\Delta t}k_s''(I+J+K)^{P+\Delta t}}{l''}} \tag{B34a}$$

$$YZ_s = -4.5ZZ_s \tag{B34b}$$

$$XZ_s = 8ZZ_s \tag{B34c}$$

$$AZ_s = -YZ_s \tag{B34d}$$

$$BZ_s = \left[6\alpha_2''(I+J+K)^{P+\Delta t}(\Delta x'')^2 - 9\right]ZZ_s - \frac{1}{\Delta t}$$

$$- \frac{\sigma\epsilon_s''\left[T_s(I+J+K)^{P+\Delta t}\right]^3\left[\alpha_1''(I+J+K)^{P+\Delta t} + \frac{11}{6\Delta x''}\right]}{2\left\{\rho_{HSP}\hat{C}_{p,HSP}l_{HSP}\left[\alpha_1''(I+J+K)^{P+\Delta t} + \frac{11}{6\Delta x''}\right] - \frac{\alpha_4(I+J+K)^{P+\Delta t}k_s''(I+J+K)^{P+\Delta t}}{l''}\right\}} \tag{B34e}$$

$$DZ_S = -\frac{\alpha_1''(I+J+K)^{P+\Delta t}+\frac{11}{6\Delta x''}}{2\left\{\rho_{HSP}\hat{C}_{p,HSP}l_{HSP}\left[\alpha_1''(I+J+K)^{P+\Delta t}+\frac{11}{6\Delta x''}\right]-\frac{\alpha_4''(I+J+K)^{P+\Delta t}k_s''(I+J+K)^{P+\Delta t}}{l''}\right\}}$$

$$\times\left[q_B^{P+\Delta t}+\frac{\alpha_3''(I+J+K)^{P+\Delta t}k_s''(I+J+K)^{P+\Delta t}/l''}{\alpha_1''(I+J+K)^{P+\Delta t}+\frac{11}{6\Delta x''}}\right]$$

$$-\frac{\alpha_1''(I+J+K)^{P}+\frac{11}{6\Delta x''}}{2\left\{\rho_{HSP}\hat{C}_{p,HSP}l_{HSP}\left[\alpha_1''(I+J+K)^{P}+\frac{11}{6\Delta x''}\right]-\frac{\alpha_4(I+J+K)^{P}k_s''(I+J+K)^{P}}{l''}\right\}}$$

$$\times\left(q_B^{P}+\frac{\alpha_3''(I+J+K)^{P}k_s''(I+J+K)^{P}/l''}{\alpha_1''(I+J+K)^{P}+\frac{11}{6\Delta x''}}+\frac{k_s''(I+J+K)^{P}/l''}{\alpha_1''(I+J+K)^{P}+\frac{11}{6\Delta x''}}\right.$$

$$\times\left\{\frac{1}{6(\Delta x'')^2}T_S(I+J+K)^{P}-\frac{3}{4(\Delta x'')^2}T_S(I+J+K-3)^{P}+\frac{4}{3(\Delta x'')^2}T_S(I+J+K-2)^{P}\right.$$

$$\left.\left.+\frac{3}{4(\Delta x'')^2}T_S(I+J+K-1)^{P}-\left[\frac{3}{2(\Delta x'')^2}-\alpha_2''(I+J+K)^{P}\right]T_S(I+J+K)^{P}\right\}\right.$$

$$\left.-\sigma\epsilon_s''\left[T_S(I+J+K)^{P}\right]^4\right)-\frac{1}{\Delta t}T_S(I+J+K)^{P} \qquad \text{(B34f)}$$

Char-Layer Porosity Equation

The differential equation for the char-layer porosity is

$$\frac{\partial}{\partial x}\eta+E_1\eta+E_2+E_3\frac{\partial\eta}{\partial t}=0 \qquad \text{(B35)}$$

The procedure to this point has been to approximate the first-order derivative by a central-difference approximation. With that method the diagonal element of the coefficient matrix would be $E_1^{P+\Delta t} + \frac{E_3^{P+\Delta t}}{\Delta t}$, where E_1 and E_3 are usually very small compared with the off-diagonal coefficients. One requirement for a coefficient matrix to be well conditioned is that the diagonal elements be of the same order in size as the off-diagonal elements. Therefore, to overcome the problem of a near zero diagonal, the first derivative is approximated by a three-point forward difference expression, part of which contributes to the diagonal term. Thus

$$\left(\frac{\partial \eta}{\partial x}\right)_N = \frac{-3\eta(N) + 4\eta(N+1) - \eta(N+2)}{2\Delta x} \tag{B36}$$

which is accurate to terms of the order Δx^2.

Combining equations (B35) and (B36) gives

$$\left[E_1(N) - \frac{3}{2\Delta x}\right]\eta(N) + \frac{2}{\Delta x}\eta(N+1) - \frac{1}{2\Delta x}\eta(N+2) + E_2(N) + E_3(N)\left(\frac{\partial \eta}{\partial t}\right)_N = 0 \tag{B37}$$

which yields the following modified implicit finite-difference equation

$$B(N)\,\eta(N)^{P+\Delta t} + C(N)\,\eta(N+1)^{P+\Delta t} + E(N)\,\eta(N+2)^{P+\Delta t} = D(N) \tag{B38}$$

where

$$B(N) = \frac{1}{2\Delta t}\left[E_3(N)^P + E_3(N)^{P+\Delta t}\right] + \frac{1}{2}\left[E_1(N)^{P+\Delta t} - \frac{3}{2\Delta x}\right] \tag{B39a}$$

$$C(N) = \frac{1}{\Delta x} \tag{B39b}$$

$$E(N) = -\frac{1}{4\Delta x} \tag{B39c}$$

$$D(N) = -\frac{1}{2}\left[E_2(N)^P + E_2(N)^{P+\Delta t}\right] - \frac{1}{2}\left\{E_1(N)^P - \frac{3}{2\Delta x} - \frac{1}{\Delta t}\left[E_3(N)^P + E_3(N)^{P+\Delta t}\right]\right\}\eta(N)^P$$

$$- \frac{1}{\Delta x}\eta(N+1)^P + \frac{1}{4\Delta x}\eta(N+2)^P \qquad \text{(B39d)}$$

Equation (B37) is valid at all stations from $N = 1$ to $N = I - 2$. At $N = I - 1$ the third term in equation (B37) would contain $\eta(I + 1)$ which is not defined. The finite-difference equation for station $I - 1$ is obtained in a manner similar to that used to obtain equation (B37) except that the first-order derivative is approximated by a two-point forward difference equation. Thus

$$\left(\frac{\partial \eta}{\partial x}\right)_{N=I-1} = \frac{\eta(I) - \eta(I-1)}{\Delta x} \qquad \text{(B40)}$$

which is accurate to terms of the order Δx. The resulting modified implicit finite-difference equation for station $I - 1$ is

$$B(I-1)\,\eta(I-1)^{P+\Delta t} + C(I-1)\,\eta(I)^{P+\Delta t} = D(I-1) \qquad \text{(B41)}$$

where

$$B(I-1) = \frac{1}{\Delta t}\left[E_3(I-1)^P + E_3(I-1)^{P+\Delta t}\right] + E_1(I-1)^{P+\Delta t} - \frac{1}{\Delta x} \qquad \text{(B42a)}$$

$$C(I-1) = \frac{1}{\Delta x} \qquad \text{(B42b)}$$

$$D(I-1) = -\left[E_2(I-1)^P + E_2(I-1)^P\right] - \left\{E_1(I-1)^P - \frac{1}{\Delta x} - \frac{1}{\Delta t}\left[E_3(I-1)^P + E_3(I-1)^{P+\Delta t}\right]\right\}\eta(I-1)^P - \frac{1}{\Delta x}\eta(I)^P \qquad \text{(B42c)}$$

The single boundary condition for the char-layer porosity equation is

$$\eta(I) = \eta_I \tag{B43}$$

Pyrolysis-Gas Temperature Equation

The differential equation for the pyrolysis-gas temperature is

$$\frac{\partial T}{\partial x} + \beta_1 T + \beta_2 + \beta_3 \frac{\partial T}{\partial t} = 0 \tag{B44}$$

The single boundary condition for this equation is

$$T(I) = T_s(I) \tag{B45}$$

The forms of the pyrolysis-gas temperature equation and its boundary conditions are identical to the char-layer porosity equation and boundary condition; therefore, the modified implicit finite-difference equation for pyrolysis-gas temperature is of the same form as the equations for char-layer porosity. Thus for $1 \leqq N \leqq I - 2$

$$B(N)\, T(N)^{P+\Delta t} + C(N)\, T(N+1)^{P+\Delta t} + E(N)\, T(N+2)^{P+\Delta t} = D(N) \tag{B46}$$

where

$$B(N) = \frac{1}{2\Delta t}\left[\beta_3(N)^P + \beta_3(N)^{P+\Delta t}\right] + \frac{1}{2}\left[\beta_1(N)^{P+\Delta t} - \frac{3}{2\Delta x}\right] \tag{B47a}$$

$$C(N) = \frac{1}{\Delta x} \tag{B47b}$$

$$E(N) = -\frac{1}{4\Delta x} \tag{B47c}$$

$$D(N) = -\frac{1}{2}\left[\beta_2(N)^P + \beta_2(N)^{P+\Delta t}\right] - \frac{1}{2}\left\{\beta_1(N)^P - \frac{3}{2\Delta x} - \frac{1}{\Delta t}\left[\beta_3(N)^P + \beta_3(N)^{P+\Delta t}\right]\right\} T(N)^P$$

$$- \frac{1}{\Delta x}\, T(N+1)^P + \frac{1}{4\Delta x}\, T(N+2)^P \tag{B47d}$$

and for $N = I - 1$

$$B(I - 1)\, T(I - 1)^{P+\Delta t} + C(I - 1)\, T(I)^{P+\Delta t} = D(I - 1) \tag{B48}$$

where

$$B(I - 1) = \frac{1}{\Delta t}\left[\beta_3(I - 1)^{P} + \beta_3(I - 1)^{P+\Delta t}\right] + \beta_1(I - 1)^{P+\Delta t} - \frac{1}{\Delta x} \tag{B49a}$$

$$C(I - 1) = \frac{1}{\Delta x} \tag{B49b}$$

$$D(I - 1) = -\left[\beta_2(I - 1)^{P} + \beta_2(I - 1)^{P+\Delta t}\right] - \left\{\beta_1(I - 1)^{P} - \frac{1}{\Delta x} - \frac{1}{\Delta t}\left[\beta_3(I - 1)^{P} + \beta_3(I - 1)^{P+\Delta t}\right]\right\} T(I - 1)^{P} - \frac{1}{\Delta x}\, T(I)^{P} \tag{B49c}$$

At $N = I$

$$T(I) = T_s(I) \tag{B50}$$

Pyrolysis-Gas Pressure Equation

The differential equation for the pyrolysis-gas pressure is

$$\frac{\partial^2 P^2}{\partial x^2} + \gamma_1 \frac{\partial P^2}{\partial x} + \gamma_2 P^2 + \gamma_3 + \gamma_4 \frac{\partial P^2}{\partial t} = 0 \tag{B51}$$

The form of this equation is identical to that of the solid-phase temperature equation. At interior stations the modified implicit finite-difference equations for the pyrolysis-gas pressure are

$$A_p(N)\, P^2(N - 1)^{P+\Delta t} + B_p(N)\, P^2(N)^{P+\Delta t} + C_p(N)\, P^2(N + 1)^{P+\Delta t} = D_p(N) \tag{B52}$$

where

$$A_P(N) = \frac{1}{\Delta x^2} - \frac{\gamma_1(N)^{P+\Delta t}}{2\Delta x} \tag{B53a}$$

$$B_P(N) = \gamma_2(N)^{P+\Delta t} - \frac{2}{\Delta x^2} + \frac{1}{\Delta t}\left[\gamma_4(N)^P + \gamma_4(N)^{P+\Delta t}\right] \tag{B53b}$$

$$C_P(N) = \frac{1}{\Delta x^2} + \frac{\gamma_1(N)^{P+\Delta t}}{2\Delta x} \tag{B53c}$$

$$D_P(N) = -\gamma_3(N)^P - \gamma_3(N)^{P+\Delta t} - \left[\frac{1}{\Delta x^2} - \frac{\gamma_1(N)^P}{2\Delta x}\right]P^2(N-1)^P - \left\{\gamma_2(N)^P - \frac{2}{\Delta x^2} - \frac{1}{\Delta t}\left[\gamma_4(N)^P + \gamma_4(N)^{P+\Delta t}\right]\right\}P^2(N)^P - \left[\frac{1}{\Delta x^2} + \frac{\gamma_1(N)^P}{2\Delta x}\right]P^2(N+1)^P \tag{B53d}$$

The boundary condition at the front surface (N = 1) is

$$P^2(1) = P_w^2 \tag{B54}$$

The condition at the pyrolysis zone (N = I) is

$$\left(\frac{\partial P^2}{\partial x}\right)_{N=I} = 2R_u \ell \left(\frac{\mu T}{K\bar{M}}\right)_{N=I} \dot{m}_g \tag{B55}$$

This equation is combined with equation (B51) to obtain

$$PX\ P^2(I-4)^{P+\Delta t} + PY\ P^2(I-3)^{P+\Delta t} + PZ\ P^2(I-2)^{P+\Delta t} + AP\ P^2(I-1)^{P+\Delta t} + BP\ P^2(I)^{P+\Delta t} = DP \tag{B56}$$

where

$$PX = \frac{1}{12\Delta x^2} \tag{B57a}$$

$$PY = -\frac{3}{8\Delta x^2} \tag{B57b}$$

$$PZ = \frac{2}{3\Delta x^2} \tag{B57c}$$

$$AP = -PY \tag{B57d}$$

$$BP = \frac{1}{2\Delta t}\left[\gamma_4(I)^P + \gamma_4(I)^{P+\Delta t}\right] + \frac{1}{2}\left[\gamma_2(I)^{P+\Delta t} - \frac{3}{2\Delta x^2}\right] \tag{B57e}$$

$$DP = -\frac{1}{2}\left[\gamma_3(I)^P + \gamma_3(I)^{P+\Delta t}\right] - \left[\frac{11}{6\Delta x} + \gamma_1(I)^P\right] R_u l^P \dot{m}_g^P \left(\frac{\mu T}{K\bar{M}}\right)_{N=I}^P - \left[\frac{11}{6\Delta x}\right.$$

$$\left. + \gamma_1(I)^{P+\Delta t}\right] R_u l^{P+\Delta t} \dot{m}_g^{P+\Delta t} \left(\frac{\mu T}{K\bar{M}}\right)_{N=I}^{P+\Delta t} - \frac{1}{12\Delta x^2} P^2(I-4)^P + \frac{3}{8\Delta x^2} P^2(I-3)^P$$

$$- \frac{2}{3\Delta x^2} P^2(I-2)^P - \frac{3}{8\Delta x^2} P^2(I-1)^P - \frac{1}{2}\left\{\gamma_2(I)^P - \frac{3}{2\Delta x^2} - \frac{1}{\Delta t}\left[\gamma_4(I)^P\right.\right.$$

$$\left.\left. + \gamma_4(I)^{P+\Delta t}\right]\right\} P^2(I)^P \tag{B57f}$$

Chemical-Species Conservation Equation

The differential equation for conservation of chemical species is

$$\frac{\partial}{\partial x}\dot{m}_i + \Delta_{1,i}\dot{m}_i + \Delta_{2,i} + \Delta_{3,i}\frac{\partial \dot{m}_i}{\partial t} = 0 \tag{B58}$$

The boundary condition is

$$\left(\dot{m}_i\right)_{N=I} = -M_i\left(\frac{x_i}{\eta\bar{M}}\right)_{N=I} \dot{m}_g \tag{B59}$$

Equation (B59) and its boundary condition are of the same form as the first-order equations and boundary conditions handled previously. The modified implicit finite-difference equation for conservation of chemical species for $1 \leqq N \leqq I - 2$ is

$$B_i(N)\ \dot{m}_i(N)^{P+\Delta t} + C_i(N)\ \dot{m}_i(N+1)^{P+\Delta t} + E_i(N)\ \dot{m}_i(N+2)^{P+\Delta t} = D_i(N) \tag{B60}$$

where

$$B_i(N) = \frac{1}{2\Delta t}\left[\Delta_{1,i}(N)^P + \Delta_{1,i}(N)^{P+\Delta t}\right] + \frac{1}{2}\left[\Delta_{1,i}(N)^{P+\Delta t} - \frac{3}{2\Delta x}\right] \tag{B61a}$$

$$C_i(N) = \frac{1}{\Delta x} \tag{B61b}$$

$$E_i(N) = -\frac{1}{4\Delta x} \tag{B61c}$$

$$D_i(N) = -\frac{1}{2}\left[\Delta_{2,i}(N)^P + \Delta_{2,i}(N)^{P+\Delta t}\right] - \frac{1}{2}\left\{\Delta_{1,i}(N)^P - \frac{3}{2\Delta x} - \frac{1}{\Delta t}\left[\Delta_{3,i}(N)^P + \Delta_{3,i}(N)^{P+\Delta t}\right]\right\}\dot{m}_i(N)^P - \frac{1}{\Delta x}\dot{m}_i(N+1)^P + \frac{1}{4\Delta x}\dot{m}_i(N+2)^P \tag{B61d}$$

For $N = I - 1$, the equation is

$$B_i(I-1)\ \dot{m}_i(I-1)^{P+\Delta t} + C_i(I-1)\ \dot{m}_i(I)^{P+\Delta t} = D_i(I-1) \tag{B62}$$

where

$$B_i(I-1) = \frac{1}{\Delta t}\left[\Delta_{3,i}(I-1)^P + \Delta_{3,i}(I-1)^{P+\Delta t}\right] + \Delta_{1,i}(I-1)^{P+\Delta t} - \frac{1}{\Delta x} \tag{B63a}$$

$$C_i(I - 1) = \frac{1}{\Delta x} \tag{B63b}$$

$$D_i(I - 1) = -\Delta_{2,i}(I - 1)^P - \Delta_{2,i}(I - 1)^{P+\Delta t} - \left\{ \Delta_{1,i}(I - 1)^P - \frac{1}{\Delta x} - \frac{1}{\Delta t}\left[\Delta_{3,i}(I - 1)^P + \Delta_{3,i}(I - 1)^P \right] \right\} \dot{m}_i(I - 1)^P - \frac{1}{\Delta x} \dot{m}_i(I)^P \tag{B63c}$$

For $N = I$

$$\dot{m}_i(I) = -M_i \left(\frac{x_i}{\eta \bar{M}} \right)_{N=I} \dot{m}_g \tag{B64}$$

APPENDIX C

EXACT SOLUTIONS

Pressure Distribution for a Constant Property, Incompressible, Isothermal Fluid Flowing Through an Isothermal Slab

The differential equation and boundary and initial conditions for the pyrolysis-gas pressure in the char layer are

$$\frac{\partial^2}{\partial x^2}(P^2) + \gamma_1 \frac{\partial}{\partial x}(P^2) + \gamma_2 P^2 + \gamma_3 + \gamma_4 \frac{\partial}{\partial t}(P^2) = 0 \tag{C1}$$

$$P^2 = P_w^2 \qquad (x = 0) \tag{C2}$$

$$\frac{\partial}{\partial x}(P^2) = 2\ell R_u \left(\frac{\mu T}{K\bar{M}}\right)\dot{m}_g \qquad (x = 1) \tag{C3}$$

and

$$P^2 = P_w^2 \qquad (t = 0) \tag{C4}$$

The coefficients in equation (C1) are not constant.

Equation (C1) written for the idealized case of flow of a constant property, incompressible fluid through an isothermal slab with the fluid and slab in thermal equilibrium reduces to the Laplace equation. The solution of the Laplace equation subject to the boundary conditions of equations (C2) and (C3) is

$$P = \left(\frac{2\mu\ell R_u T \dot{m}_g}{K\bar{M}} x + P_w^2\right)^{1/2} \tag{C5}$$

Transient Temperature Response of a Constant Property, Incompressible Fluid Flowing Through an Isothermal Slab

The differential equation for constant property, incompressible flow from a reservoir of specified temperature through an isothermal slab is

$$\frac{\partial \phi}{\partial x'} + A\phi + \frac{\partial \phi}{\partial t} = 0 \tag{C6}$$

The boundary condition is

$$\phi(l/v,t) = 1 \tag{C7a}$$

and the initial condition is

$$\phi(x',0) = 0 \tag{C7b}$$

where

$$\phi = \frac{T - T_s}{T_o - T_s} \tag{C8a}$$

and

$$x' = xl/v \tag{C8b}$$

To solve this set of equations the Laplace transform of ϕ defined by

$$P = \int_0^\infty e^{-St}\phi(x',t)dt \tag{C9}$$

is introduced. Equations (C6) and (C7) become

$$\frac{\partial P}{\partial x'} + (A + S)P = 0 \tag{C10}$$

$$P(l/v,t) = 1.0/S \tag{C11a}$$

and

$$P(x',0) = 0 \tag{C11b}$$

The solution to equations (C10) and (C11) is

$$P = \frac{1}{S} \exp\left[A(l/v - x')\right]\exp\left[S(l/v - x')\right] \tag{C12}$$

The reverse transform of equation (C12) gives

$$T' = \exp\left[Al/v(1 - x)\right]S_x(t) \tag{C13a}$$

where

$$S_x(t) = \begin{cases} 0 & \left(0 < t < (x - 1)l/v\right) \\ 1 & \left(t > (x - 1)l/v\right) \end{cases} \tag{C13b}$$

Transient Response of a Heat Sink Subjected to a Suddenly Applied Constant Heating Rate

The exact solution for the temperature response of a flat plate subjected to a suddenly applied constant heating rate is given in reference 15. When written with the symbols used in this paper, the equation is

$$T_s = T_{s,0} + q\frac{l + l'}{k_s}\left\{\frac{k_s t}{\rho_s \hat{C}_{p,s}(l + l')^2} + \frac{1}{2}(1 - x)^2 - \frac{1}{6}\right.$$

$$\left. - \frac{2}{\pi^2}\sum_n \frac{(-1)^n}{n^2}\cos\left[n\pi(1 - x)\right]\exp\left[\frac{n^2\pi^2 k_s t}{\rho_s \hat{C}_{p,s}(l + l')^2}\right]\right\} \tag{C14}$$

Quasi-Steady-State Ablation Case

A quasi-steady-state ablating system is one in which the pyrolysis interface and the front surface recede at the same rate; that is, the char thickness is constant. If in addition the pyrolysis gases are inert, incompressible, and in local thermal equilibrium with the char layer, material properties of the system are uniform and independent of temperature, there are no energy sources, viscous dissipation, or diffusion, and conditions exist such that no energy is transferred into the uncharred layer, an exact solution to the governing mathematical equations can be obtained.

The equation governing the char-layer temperature is (eqs. (A18) and (A19))

$$(1-\eta)\frac{\rho_s C_{p,s}}{M_s}\left(\frac{\partial T_s}{\partial t} - V_c\frac{\partial T_s}{\partial x}\right) = \frac{k_s}{l^2}\frac{\partial^2 T_s}{\partial x^2} + \frac{1}{l^2}\frac{\partial k_s}{\partial x}\frac{\partial T_s}{\partial x} - H_A\left(T_s - T\right) + \eta R_s\left[H(T)\right]_s$$

$$+ \eta R_{h,s} H_s - \eta\sum_r r_h^{(r)}\Delta H^{(r)} + (1-\eta)(A-E)$$

$$+ (1-\eta)q_s''' + \frac{\rho_s H_s}{M_s}\left(\frac{\partial \eta}{\partial t} - V_c\frac{\partial \eta}{\partial x}\right) \qquad \text{(C15)}$$

The governing equation for the pyrolysis-gas temperature is (eqs. (A34) and (A35))

$$\eta\left(\frac{v}{l} - V_c\right)\left(\sum_i \frac{\rho_i C_{p,i}}{M_i} - R_u\sum_i\frac{\rho_i}{M_i}\right)\frac{\partial T}{\partial x} - H_A\left(T_s - T\right) - \eta R_u\left[\frac{\rho}{\eta\bar{M}}\left(\frac{\partial \eta}{\partial t} - V_c\frac{\partial \eta}{\partial x}\right) + \frac{\partial}{\partial t}\left(\sum_i\frac{\rho_i}{M_i}\right)\right.$$

$$\left. + \left(\frac{v}{l} - V_c\right)\frac{\partial}{\partial x}\left(\sum_i\frac{\rho_i}{M_i}\right)\right]T + \eta\sum_i R_{T,i}H_i - \eta\frac{v^2}{2}\sum_i R_{T,i}M_i + \eta R_s\left[H(T)\right]_s + \eta R_{h,s}H_s$$

$$- \eta\sum_r r_h^{(r)}\Delta H^{(r)} + \eta\left(\sum_i\frac{\rho_i C_{p,i}}{M_i} - R_u\sum_i\frac{\rho_i}{M_i}\right)\frac{\partial T}{\partial t} = 0 \qquad \text{(C16)}$$

With quasi-steady-state ablation, l, $\dot{m}_p$, and $\dot{m}_s$ are constant and

$$\left.\begin{aligned} \frac{\dot{m}_g}{\Delta\rho} &= \frac{\dot{m}_s}{\rho_{s,0}} \\ \frac{\partial T_s}{\partial t} &= 0 \\ \frac{\partial T}{\partial t} &= 0 \end{aligned}\right\} \qquad \text{(C17)}$$

By using equation (C17) with the assumptions of no chemical reactions, incompressible pyrolysis gases, constant material properties, and no energy sources or sinks, equations (C15) and (C16) reduce to

$$\frac{\partial^2 T_s}{\partial x^2} + \frac{l}{k_s} \hat{C}_{p,s} \dot{m}_s \frac{\partial T_s}{\partial x} - \frac{l^2}{k_s} H_A \left(T_s - T \right) = 0 \tag{C18}$$

and

$$\eta \left(\frac{v}{l} - \frac{\dot{m}_s}{\rho_{s,0} l} \right) \left(\rho \hat{C}_p - R_u \sum_i \frac{\rho_i}{M_i} \right) \frac{\partial T}{\partial x} - H_A \left(T_s - T \right) = 0 \tag{C19}$$

Equations (C18) and (C19) are combined to eliminate the term $H_A \left(T_s - T \right)$; thus

$$\frac{\partial^2 T_s}{\partial x^2} + \frac{l}{k_s} \left[\hat{C}_{p,s} \dot{m}_s \frac{\partial T_s}{\partial x} - \eta \left(v - \frac{\dot{m}_s}{\rho_{s,0}} \right) \left(\rho \hat{C}_p - R_u \sum_i \frac{\rho_i}{M_i} \right) \frac{\partial T}{\partial x} \right] = 0 \tag{C20}$$

Invoking the assumption of local thermal equilibrium between the pyrolysis gases and char layer $\left(T = T_s \text{ and } \frac{\partial T}{\partial x} = \frac{\partial T_s}{\partial x} \right)$ gives

$$\frac{\partial^2 T_s}{\partial x^2} + D \frac{\partial T_s}{\partial x} = 0 \tag{C21}$$

where

$$D = \frac{l}{k_s} \left[\dot{m}_s \hat{C}_{p,s} + \left(\dot{m}_g + \eta \frac{\rho \dot{m}_s}{\rho_{s,0}} \right) \left(\hat{C}_p - \frac{R_u}{\overline{M}} \right) \right] \tag{C22}$$

The solution of equation (C21) is

$$T_s = C_1 + C_2 \exp(-Dx) \tag{C23}$$

The integration constants are determined from the boundary conditions

$$\left.\begin{aligned} T_s(0) &= \overline{T}_1 \\ T_s(I) &= \overline{T}_I \end{aligned}\right\} \tag{C24}$$

and the final solution is

$$T_s = \frac{\overline{T}_I - \overline{T}_1 \exp(-D) + \left(\overline{T}_1 - \overline{T}_I\right)\exp(-Dx)}{1 - \exp(-D)} \tag{C25}$$

The mass loss rates $\dot{m}_s$ and $\dot{m}_g$ and the char-layer thickness l are obtained from equation (C25) and the following equations

$$\left.\begin{aligned} \frac{\dot{m}_g}{\Delta\rho} &= \frac{\dot{m}_s}{\rho_{s,0}} \\ \left(\frac{\partial T_s}{\partial x}\right)_{x=0} &= \frac{l}{k_s}\left(\dot{m}_s H_c - q_{AERO}\right) \\ \left(\frac{\partial T_s}{\partial x}\right)_{x=1} &= -\dot{m}_g \Delta H_p \frac{l}{k_s} \end{aligned}\right\} \tag{C26}$$

where energy transfer into the uncharred layer is neglected. Thus

$$\left.\begin{aligned} \dot{m}_s &= \frac{\rho_{s,0}/\Delta\rho q_{AERO}}{H_c + \Delta H_p + D'\left(\overline{T}_1 - \overline{T}_I\right)} \\ \dot{m}_g &= \frac{q_{AERO}}{H_c + \Delta H_p + D'\left(\overline{T}_1 - \overline{T}_I\right)} \\ l &= \frac{k_s}{q_{AERO} D'}\left[H_c + \Delta H_p + D'\left(\overline{T}_1 - \overline{T}_I\right)\right]\ln\left[\frac{\Delta H_p + D'\left(\overline{T}_1 - \overline{T}_I\right)}{\Delta H_p}\right] \end{aligned}\right\} \tag{C27a}$$

where

$$D' = \hat{C}_{p,s} + \left(\hat{C}_p - \frac{R_u}{\overline{M}}\right)\left(\frac{\Delta\rho - \eta\rho}{\rho_{s,0}}\right) \tag{C27b}$$

REFERENCES

1. Price, R. E.; and Schultz, F. E.: Modification of the One-Dimensional REKAP Program To Allow for Charring in Three Material Layers. GE-RS 69SD420 (Contract NAS 3-10285), General Electric Co., Jan. 1969. (Available as NASA CR-72488.)

2. Wells, P. B.: A Method for Predicting the Thermal Response of Charring Ablation Materials. Doc. No. D2-23256, Boeing Co., 1964.

3. Moyer, Carl B.; Anderson, Larry W.; and Dahm, Thomas J.: A Coupled Computer Code for the Transient Thermal Response and Ablation of Non-Charring Heat Shields and Nose Tips. NASA CR-1630, 1970.

4. Swann, Robert T.; Pittman, Claud M.; and Smith, James C.: One-Dimensional Numerical Analysis of the Transient Response of Thermal Protection Systems. NASA TN D-2976, 1965.

5. Clark, Ronald K.: Flow of Hydrocarbon Gases in Porous Media at Elevated Temperatures. M.A.E. Thesis, Univ. of Virginia, Aug. 1968.

6. Clark, Ronald K.: Simulation of Pyrolysis-Gas Flow Through a Char Layer During Ablation. NASA TN D-5464, 1969.

7. Stroud, C. W.: A Study of the Reaction-Plane Approximation in Ablation Analyses. NASA TN D-4817, 1968.

8. Clark, Ronald Keith: A Numerical Analysis of the Transient Response of an Ablation System Including Effects of Thermal Non-Equilibrium, Mass Transfer and Chemical Kinetics. Ph. D. Thesis, Virginia Polytechnic Inst. & State Univ., May 1972.

9. Bland, D. R.: Mathematical Theory of the Flow of a Gas in a Porous Solid and of the Associated Temperature Distributions. Proc. Roy. Soc. (London), ser. A, vol. 221, no. 1144, Jan. 7, 1954, pp. 1-28.

10. Clarke, J. F.; and McChesney, M.: The Dynamics of Real Gases. Butterworths, 1964.

11. Alekseyev, B. V.: Boundary Layer and Chemical Reactions. NASA TT F-549, 1969.

12. Scheidegger, Adrian E.: The Physics of Flow Through Porous Media. Rev. ed., Macmillan Co., 1960.

13. Bruce, G. H.; Peaceman, D. W.; Rachford, H. H., Jr.; and Rice, J. D.: Calculations of Unsteady-State Gas Flow Through Porous Media. J. Petrol. Technol., vol. 5, no. 3, Mar. 1953.

14. Dow, Marvin B.; Bush, Harold G.; and Tompkins, Stephen S.: Analysis of the Supercircular Reentry Performance of a Low-Density Phenolic-Nylon Ablator. NASA TM X-1577, 1968.

15. Carslaw, H. S.; and Jaeger, J. C.: Conduction of Heat in Solids. Clarendon Press (Oxford), 1957.